5

Physical Properties of Fillers and Filled Materials

The following information is analyzed in this chapter:

- Physical properties of fillers
- The effect of physical properties of fillers on the properties of filled materials
- The universal principles governing the relationships between the properties of fillers and effect of fillers on the properties of filled materials.

Some examples are given to illustrate the nature of these relationships and the effects obtained.

5.1 DENSITY[1-15]

The data in Table 5.1 show that the range of densities of fillers is very wide ranging from 0.03 to 19.36 g/cm^3. If we allow that air can also be considered a filler and platinum may be potentially applied in conductive materials, fillers occupy the full spectrum of density of known materials. But it is apparent from the table that most fillers have densities in a range from 2 to 3 g/cm^3.

The effect of filler density on the density of filled product can be closely approximated by the additivity rule. If a more precise method of density estimation is required or filler/matrix mixtures are far from being perfect, several corrections are necessary. System density becomes nonlinear close to the critical volume concentration (CVC). The critical volume concentration determines the amount of conductive filler which rapidly increases the conductivity of the composite. Figure 5.1 shows that at, or close to the critical volume concentration, density decreases. This density difference can be detected either after the CVC (polyethylene), before (polystyrene) or the two depressions are observed – one before and one after the CVC (polymethylmethacrylate) is reached.[15] This density depression is due to filler-matrix interaction.

Table 5.1. Density of fillers

Density range, g/cm^3	**Fillers** (filler density is given in parentheses)
0.1-0.39	expanded polymeric microspheres (0.03-0.13), hollow glass beads (0.12-1.1), thin-wall, hollow ceramic spheres (0.24)
0.4-0.69	wood flour (0.4-1.35), porous ceramic spheres (0.6-1.05), silver coated glass beads (0.6-0.8)
0.7-0.99	thicker wall, hollow ceramic spheres (0.7-0.8), polyethylene fibers and particles (0.9-0.96)
1-1.99	cellulose fibers (1-1.1), unexpanded polymeric spheres (1.05-1.2), rubber particles (1.1-1.15), expanded perlite (1.2), anthracite (1.31-1.47), aramid fibers (1.44-1.45), carbon black (1.7-1.9), PAN-based carbon fibers (1.76-1.99), precipitated silica (1.9-2.1), pitch-based carbon fibers (1.9-2.25)
2-2.99	fumed and fused silica (2-2.2), graphite (2-2.25), sepiolite (2-2.3), diatomaceous earth (2-2.5), fly ash (2.1-2.2), slate flour (2.1-2.7), PTFE (2.2), calcium hydroxide (2.2-2.35), silica gel (2.2-2.6), boron nitride (2.25), pumice (2.3), attapulgite (2.3-2.4), calcium sulfate (2.3-3), ferrites (2.3-5.1), cristobalite (2.32), aluminum trihydroxide (2.4), magnesium oxide and hydroxide (2.4), unexpanded perlite (2.4), solid ceramic spheres (2.4-2.5), solid glass beads (2.46-2.54), kaolin and calcinated kaolin (2.5-2.63), silver coated glass spheres and fibers (2.5-2.8), glass fibers (2.52-2.68), feldspar (2.55-2.76), clay (2.6), hydrous calcium silicate (2.6), vermiculite (2.6), quartz ans sand (2.65), pyrophyllite (2.65-2.85), aluminum powders and flakes (2.7), talc (2.7-2.85), nickel coated carbon fiber (2.7-3), calcium carbonate (2.7-2.9), mica (2.74-3.2), zinc borate (2.8), beryllium oxide (2.85), dolomite (2.85), wollastonite (2.85-2.9), aluminum borate whiskers (2.93)
3-4.99	zinc stannate and hydroxystannate (3-3.9), silver coated aluminum powder (3.1), apatite (3.1-3.2), barium metaborate (3.3), titanium dioxide 3.3-4.25), antimony pentoxide (3.8), zinc sulfide (4), barium sulfate and barite (4-4.9), lithopone (4.2-4.3), iron oxides (4.5-5.8), sodium antimonate (4.8), silver coated inorganic flakes (4.8), molybdenum disulfide (4.8-5)
5-6.99	antimony trioxide (5.2-5.67), zinc oxide (5.6)
7-8.99	nickel powder and flakes (8.9), copper powder (8.92)
9 and above	silver coated copper powders and flakes (9.1-9.2), molybdenum powder (10.2), silver powder and flakes (10.5), gold powder (18.8), tungsten powder (19.35)

Figure 5.2 shows the influence of filler concentration on the density of polymer calculated from the following equation:

$$d_{p,p} = \frac{d_c - d_{MF} V_{MF}}{1 - V_{MF}} \qquad [5.1]$$

where

$d_{p,p}$ density of polymer
d_c density of composite
d_{MF} density of filler
V_{MF} volume fraction of filler

Below the critical concentration of filler some polymer is converted to the interphase layer where the polymer has a higher density because of closer packing,

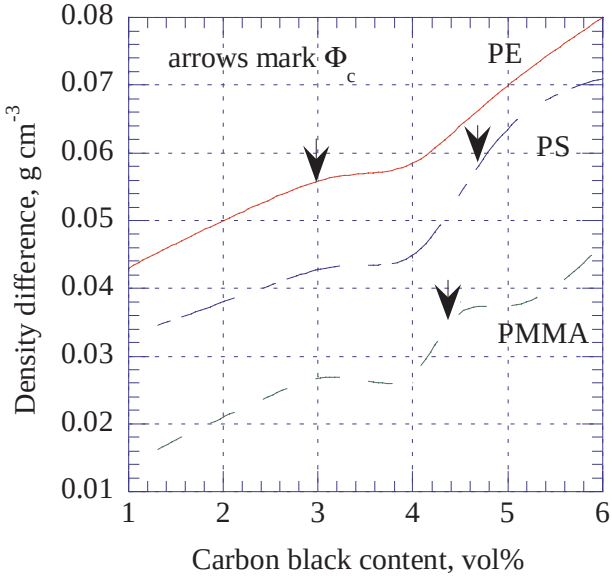

Figure 5.1. Density of composite vs. concentration of carbon black around the CVC. [Data from Weeling B, Electrical Conductivity in Heterogeneous Polymer Systems. Conductive Polymers, Conference Proceedings, 1992, Bristol, UK.]

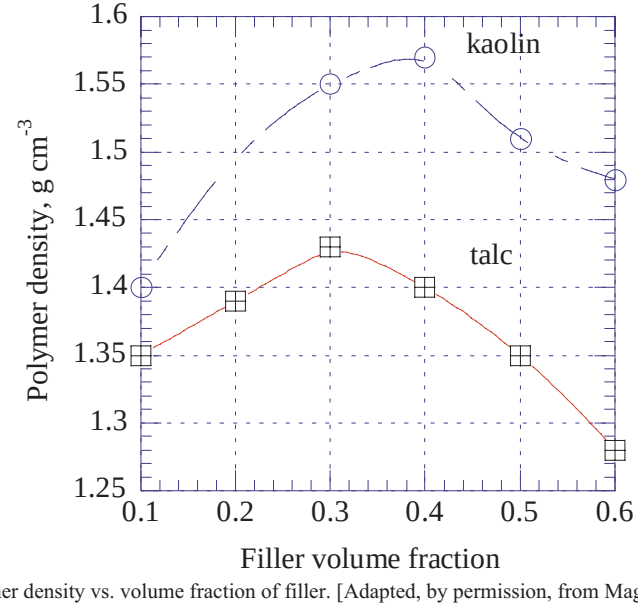

Figure 5.2. Polymer density vs. volume fraction of filler. [Adapted, by permission, from Magrupov M A, Umarov A V, Saidkhodzhaeva K S, Kasimov G A, *Int. Polym. Sci. Technol.*, **23**, No.1, 1996, T/77-9.]

therefore the density of the polymer increases. Above the critical concentration of filler, there is not enough polymer to cover the surface which increases the free volume and the density of the composite decreases.[10]

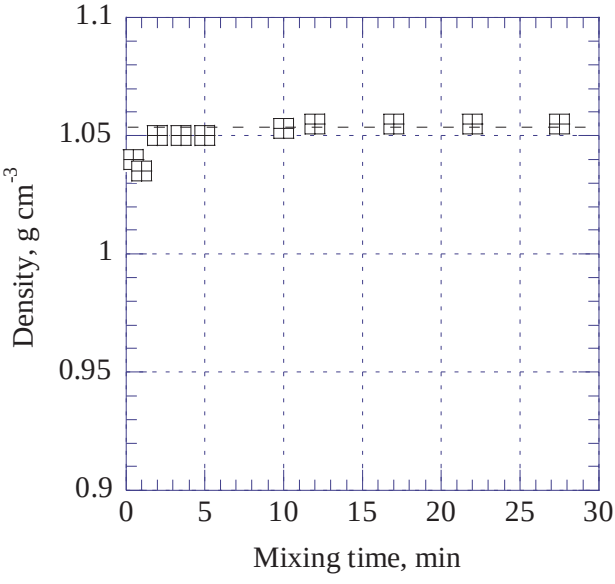

Figure 5.3. Density of SBR containing 30 phr carbon black vs. mixing time. [Adapted, by permission, from Clarke J, Freakley P K, *Rubb. Chem. Technol*., **67**, No.4, 1994, 700-15.]

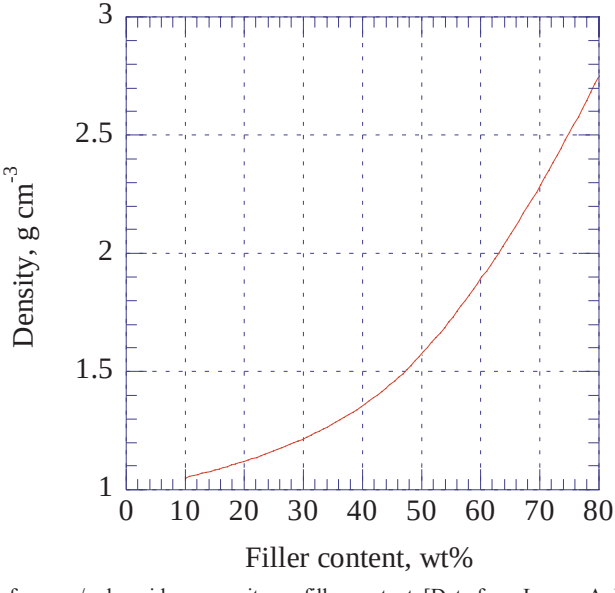

Figure 5.4. Density of copper/polyamide composite vs. filler content. [Data from Larena A, Pinto G, *Polym. Composites*, **16**, No.6, 1995, 536-41.]

Figure 5.3 shows the effect of mixing on the density of composite. The line gives the theoretical density of the composite calculated by the additivity rule. The density of composite at 0 mixing time was calculated assuming that the DBPA

value for carbon black was equivalent to the air content of the carbon black pellets. The graph shows that the ultimate density is approached at a very early stage of the mixing process.

Composite density can be expected to vary because of the uneven distribution of filler particles in the manufactured product. This is very typical of the injection molding process where filler is distributed in a complex pattern of flow. In glass reinforced polystyrene parts, manufactured by injection molding, the density varied between 0.9 and 1.4 g/cm^3 depending on the process conditions and locations from which the sample was taken.[7]

The other reason for variable density is traced to air voids in the material, related to the method of filler incorporation. Figure 5.4 shows the relationship of recorded densities for copper particles of different sizes in polyamide. The particle size did not have an influence. The variations were related to incorporation methods and filler content. The lines show calculated densities at different void volume contents. The void volume content varied between 10 and 20%.[8]

5.2 PARTICLE SIZE[16-46]

According to the data in Table 5.2, only primary particles of fumed and precipitated silica and ultrafine titanium dioxide are produced in sizes lower than 10 nm. The next group includes nanoparticles which are manufactured by chemical methods and metal evaporation techniques combined with oxidation. Mineral fillers of the smallest particle sizes belong to the group of particles with a size above 100 nm. All pigments also belong to the same group (0.1-0.5 μm) together with some synthetic fillers. Metal powders have still larger particles above 0.5 μm. The fillers used in the largest quantities have particles in the range of 1-10 μm. The largest particles are produced for materials used either for decoration (e.g., sand in stucco), as an inexpensive products (e.g., sand in unsaturated polyester composites), or are composed of materials difficult to pulverize (rubber particles).

It is apparent from the data that particles of a few nanometers in size can only be made on industrial scale by synthetic methods. On the other hand, these particles are either intentionally or unintentionally aggregated and agglomerated in their powder forms. Thus, for the dispersion of fillers, agglomerate and aggregate size is usually as relevant as the primary particle size. Fillers, which are obtained by various milling and classification processes, can also be obtained in the form of small particles, but usually not below 100 nm.

The most difficult part of particle size estimation is related to the determination methods themselves. Particle size determination is complicated by size distribution, the presence of particle associations, and the shape of particles. If particles are not spherical, more than one parameter is needed to describe them and if the shape of the particle is irregular, numerous parameters are needed to express their dimensions. The method used for particle size determination (sieving, light scattering, microscopy, etc.) determines what dimensional aspects are measured. In addi-

tion, different methods are more useful than the others for the determination of particles in certain size ranges. All these procedural difficulties make it difficult to find a precise method. The more precise analysis can only be done within the scope of a well controlled experiment aimed at understanding a certain property. Particle size is, however, the one property of a filler that influences every aspect of its use and the success of many applications. In view of the fact that there is no general way of dimensioning filler particles we will deal with the particle size of specific fillers throughout the book and make no attempt here to deal with specifics.

Table 5.2. The average particle size of different fillers

Particle size range, μm	**Filler** (the range of the average particle sizes for a particular filler is given in parentheses)
below 0.01	primary particles of fumed silica (0.005-0.04), primary particles of precipitated silica (0.005-0.1), ultrafine titanium dioxide (0.008-0.04)
0.011-0.03	aluminum oxide (0.013-0.1), carbon black (0.14-0.25), precipitated calcium carbonate (0.02-0.4), colloidal antimony pentoxide (0.025-0.075), iron oxide nanoparticles (0.026)
0.031-0.06	zinc oxide (0.036-3), ferrites (0.05-14)
0.061-0.1	barium titanate (0.07-2.7)
0.1-0.5	blanc fixe (0.1-0.7), attapulgite (0.1-20), bentonite (0.18-1), titanium dioxide pigment (0.19-0.3), antimony trioxide (0.2-3), kaolin (0.2-7.3), aggregates of fumed silica (0.2-15), calcium carbonate (0.2-22), silver powders and flakes (0.25-25), zinc sulfide (0.3-0.35), ball clay (0.4-5), molybdenum disulfide (0.4-38), magnesium hydroxide (0.5-7.7)
0.6-1	zinc borate (0.6-1), lithopone (0.7), aluminum trihydroxide (0.7-55), tungsten powder (0.7-18), gold powder (0.8-9), iron oxide (0.8-10)
1-5	precipitated silica agglomerates (1-40), ceramic beads (1-50), talc (1.4-19), copper powder (1.5-5), silica gel (2-15), quartz (tripoli) (2-19), sand (2-3000), nickel powder (2.2-9), zinc stannate (2.5), barites and synthetic barium sulfates (3-30), feldspar (3.2-14), diatomaceous earth (3.7-24.6), fly ash (4), fused silica (4-28), mica (4-70), calcium hydroxide (5), sepiolite (5-7), PTFE (5-25)
6-10	unexpanded polymeric spheres (6-35), graphite (6-96), glass beads (7-8)
10-100	aluminum powder (10-23), antimony pentoxide (10-40), wood flour (10-100), perlite (11-37), expanded polymeric spheres (15-140), beryllium oxide (20), apatite (43)
above 100	porous ceramic beads (100-350), rubber particles (100-2000), coarse sand (500-3000)

5.3 PARTICLE SIZE DISTRIBUTION[17,28,30,33,35,45,47-56]

Figure 5.5 compares two grades of kaolin manufactured in a form of slurry. A medium particle size kaolin (Britefil 80 Slurry) is used in the paper industry where small particle size is not critical. Another grade of kaolin (Royal Slurry) is used in

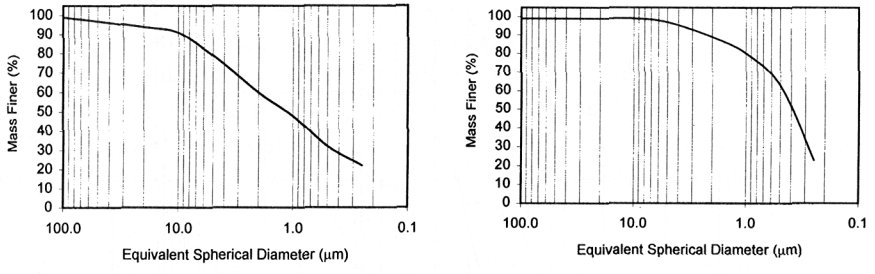

Figure 5.5. Particle size distribution of Britefil 80 Slurry (left) and Royal Slurry (right). *Courtesy of Albion Kaolin Co., Hephzibah, GA, USA.*

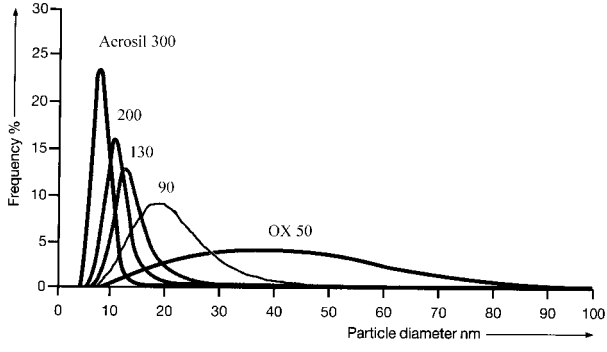

Figure 5.6. Particle size distribution of different grades of Aerosil. *Courtesy of Degussa AG, Frankfurt/Main, Germany.*

specialty applications where fine grade is needed. This grade is milled to a smaller particle size and stabilized with a dispersant. This example shows that milling technology is capable of tailoring particle size distribution to requirements.

Figure 5.6 shows that pyrogenic manufacturing gives excellent control over particle size distribution and median particle size. These grades of fumed silica differ in properties and require a different technological approaches to their dispersion since small particle size filler is more difficult to disperse. At the same time, smaller particle sizes give more transparent products and better reinforcement.

Figure 5.7 shows particle size distribution of synthetic barium sulfate. The characteristic feature of these curves is their steepness which denotes a very narrow particle size distribution which was obtained by controlling the conditions of precipitation. The development of this kind of particle size distribution in a small particle sized filler allows for substantial improvement in the gloss of coatings.

Similar benefits can be shown with the talcs presented in Figure 5.8. The following are the properties of these talcs related to their particle size distribution:

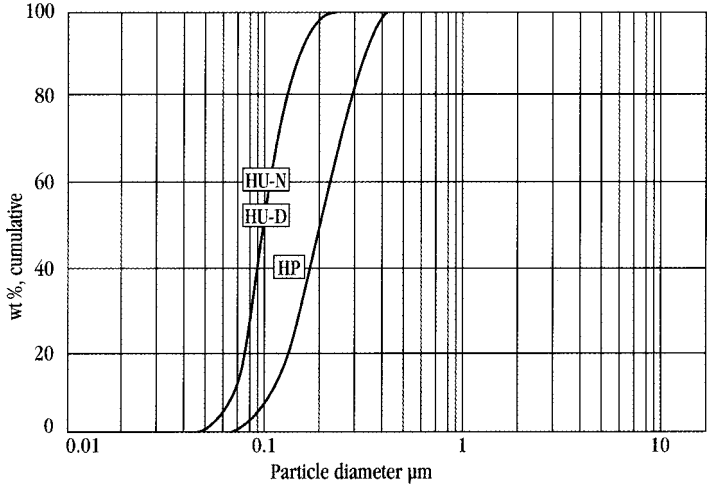

Figure 5.7. Particle size distribution of Sachtoperse. *Courtesy of Sachtleben Chemie GmbH, Duisburg, Germany.*

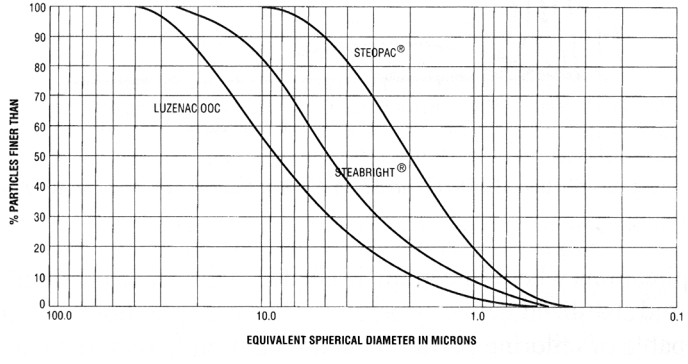

Figure 5.8. Particle size distribution of different talcs. *Courtesy of Luzenac Group, Toulouse, France.*

	Luzenac 00C	*Steabright*	*Steopac*
Whiteness, %	84.2	87.7	88.9
Oil absorption, g/100 g	35	50	62
Opacity	0.99	0.992	0.995
Matting (85° sheen)	1.4	1.8	2.8

The three talcs have the same composition (talc: 40-41%, chlorite: 57-59%). The differences in properties can be attributed to the way in which they were processed.

A general conclusion from this is that industry can manufacture a variety of particle size distributions tailored to the requirements of the application. Particle

size distribution is controlled by the technological parameters of filler production and the methods of classification as well as blending.

Graphing does not always provide the best means of comparing particle size distribution unless the materials are very divergent (as the selected examples). A mathematical form of data presentation is sometimes more convenient. Granulometry in number and in weight is calculated from the following equations:[54]

$$L_n = \frac{\sum_i d_i \times n_i}{\sum_i n_i} \qquad L_w = \frac{\sum_i d_i^2 \times n_i}{\sum_i d_i \times n_i} \qquad [5.2]$$

where:

d_i	particle diameter
n_i	number of particles

The results are either expressed as a ratio - L_w/L_n or a dispersity factor is calculated:

$$D = \frac{L_w - L_n}{L_n} \qquad [5.3]$$

In a study of the synthesis of a monodisperse colloidal silica, it was possible to control the particle size distribution.[45] A range of products was obtained with ratios L_w/L_n=1.03-33. This again shows that it is possible to tailor particle size to the requirements. We now need to determine what the ratio should be and why.

In plastic products, the particle size distribution of the filler has influence on viscosity and on the amount of filler which can be incorporated. The obvious benefits of mixing particles of different sizes are discussed below. This inevitably leads to a discussion of packing density and critical pigment volume concentration. In some plastics, a certain stress distribution is required and, in such cases, monodisperse, spherical particles are best.

Fillers may also play the role of a pigment and when they do, the particle size distribution is important for several reasons. Figure 5.9 shows that the tint strength and opacity depend particle size. This graph is based on the following relationship developed from the scattering theory of Mie:

$$d_{opt} \sim \frac{\lambda}{1.6(n_p - n_B)} [nm] \qquad [5.4]$$

where:

d_{opt}	optimum particle diameter
λ	wavelength of the incident light
n_p	refractive index of pigment
n_B	refractive index of matrix

According to this relationship there is a direct interdependence between scattering power and particle diameter. This equation suggests that pigment having different particle size distributions may have different scattering properties not only in terms

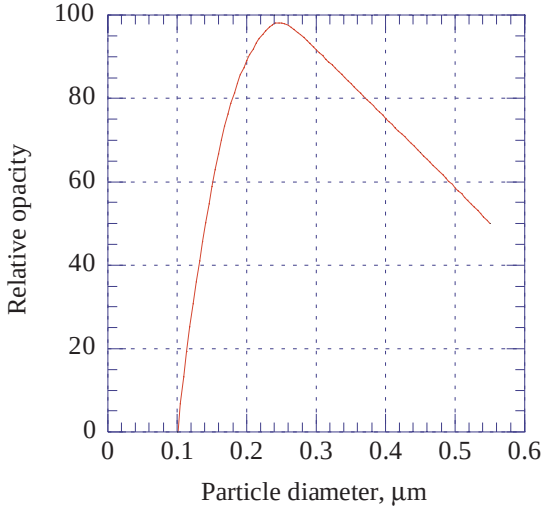

Figure 5.9. Relative opacity vs. particle diameter.

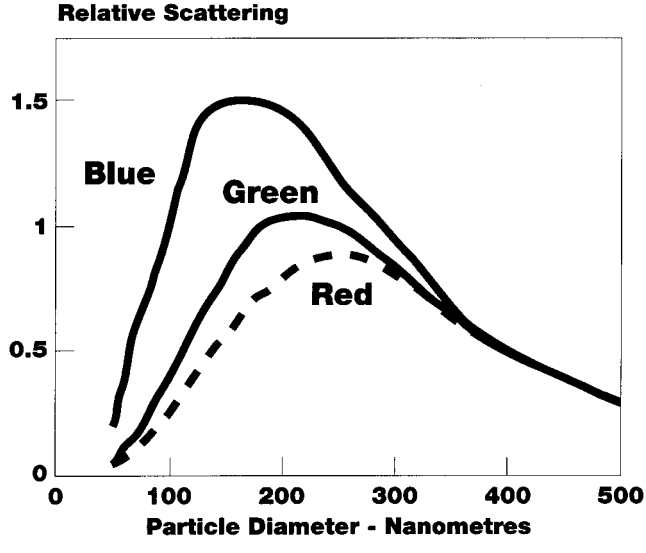

Figure 5.10. Scattering of rutile titanium dioxide. *Courtesy of Millennium Inorganic Chemicals, Auburn, Australia.*

of hiding and opacity but also may influence the color of reflected light. Figure 5.10 shows the effect of particle diameter on scattering of blue, green and red light. Changes to the particle size distribution will change the undertone of the pigment allowing a system to be tailored to the requirements. Certain grades may be capable of providing optical brightening or of masking the yellow color.

5.4 PARTICLE SHAPE[23,45,57-59]

The morphology of filler particles can be compared using the SEM and TEM micrographs included in Chapter 2. Here, only summary is included in the form of table (Table 5.3).

Table 5.3. Typical shapes of fillers particles

Shape	Filler examples
spherical	aluminum powder, aluminum oxide, carbon black, ceramic beads, copper powder, fumed silica, glass beads, silver powder, titanium dioxide, zinc oxide
cubic	calcium hydroxide, calcium hydroxide, feldspar
tabular	barite, feldspar, sand
dendritic	copper powder, nickel powder
flake	aluminum flake, graphite, kaolin, mica, perlite, tripoli, sliver flake, talc, vermiculite
elongated	aluminum borate whisker (ribbons or cylinders), aramid (fiber), attapulgite (needle), carbon fiber, cellulose fiber , glass fiber, titanium dioxide (acicular), wood flour (fiber), wollastonite (acicular)
irregular	aluminum oxide, aluminum hydroxide, anthracite, attapulgite, barite, calcium carbonate, clay, dolomite, fly ash, magnesium hydroxide, perlite, precipitated silica

Each particle shape brings with it certain advantages. Spherical particles give the highest packing density, a uniform distribution of stress, increase melt flow and powder flow, and lower viscosity. Cubic and tabular shapes give good reinforcement and packing density. Dendritic particles have a very large surface area available for interaction. Flakes have large reflecting surfaces, facilitate orientation, and lower the permeability of liquids, gases and vapors. Elongated particles give superior reinforcement, reduce shrinkage and thermal expansion and facilitate thixotropic properties. Irregular particles may not possess special advantages but they are generally easier to make and are thus inexpensive fillers. These properties are discussed in other chapters of this book.

5.5 PARTICLE SURFACE MORPHOLOGY AND ROUGHNESS[23,58,60-68]

The particle surface of mineral fillers can be estimated from a knowledge of the crystal structure, since the milling process cleaves the crystals according to a typical pattern of cleavage for a particular mineral. Many crystals, particularly these of mineral origin, cleave in only one direction and form plate like particles. Table 5.4 summarizes the crystal structure and cleavage pattern of some fillers of mineral origin.

The information in the table shows that the shape of filler particles is determined by their crystal structure and cleavage. The surface area of crystal is increased by milling but it retains the original features of the mineral. This

information can be compared with micrographs in Chapter 2. The interactions that may occur on such a filler surface depend on the crystal structure which dictates a defined pattern of chemical organization and on the functional groups which are available on the surface for the eventual reaction with the matrix.

Table 5.4. Crystal structure and cleavage pattern of selected mineral fillers

Crystal structure	**Fillers** (typical cleavage is given in parentheses)
hexagonal	apatite (indistinct in one basal direction), graphite (perfect in one direction), kaolin
monoclinic	aluminum trihydroxide (one direction), attapulgite, bentonite (perfect in one direction), calcium sulfate (one direction and distinct in two others), feldspar (good in 2 directions forming nearly right angled prisms), mica (perfect in one direction producing thin sheets or flakes), pyrophyllite (perfect in one direction), talc (perfect in one direction, basal), vermiculite
orthorhombic	barite (perfect in one direction, less so in another direction), calcium carbonate - aragonite (one direction), sepiolite
tetragonal	cristobalite (absent)
triclinic	feldspar (perfect in one and good in another direction forming nearly right angled prisms), wollastonite (perfect in two directions at near 90 degrees forming prisms with a rectangular cross-sections)
trigonal	calcium carbonate - calcite (perfect in three directions, forming rhombohedrons), dolomite (perfect in three directions forming rhombi), quartz

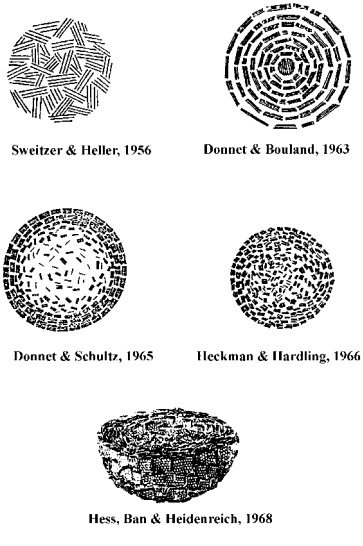

Figure 5.11. The models of carbon black particles. [Adapted, by permission, from Donnet J B, *Kaut. u. Gummi Kunst*., **47**, No.9, 1994, 628-32.]

In synthetic materials, the surface organization also depends on the internal structure of particles. Carbon black is good example. Figure 5.11 shows the models of carbon black primary particles. The most recent model developed by Hess, Ban and Heidenreich is commonly accepted as being characteristic of carbon black particles. The particle is composed of small elements which are interconnected to form quasi-spherical particles.[58] Recent studies[62] indicate that the core of the particle is less dense and filled with voids but organized in such a way that graphitic scales form on the surface which makes surface rough and accommodating to polymer chains. In a different process where

carbon and aramid fiber are formed there are also numerous imperfections on the surface.[63,65] With the advent of atomic force microscopy these imperfections can now be observed and surface roughness can be estimated in numerical form. This surface roughness is important in the development of adhesive forces between the filler and matrix.

The surface roughness of filled materials is obviously not related to filler surface imperfections but it is very much determined by the shape of filler particles.[60,64] The effect of glass fibers in plastics and flatting agents are specific examples of the influence of specific shaped particles on surface roughness.

5.6 SPECIFIC SURFACE AREA[69-80]

Specific surface area is a convenient method of characterizing fillers. The results can be correlated to many performance characteristics and to the properties of filled systems. Table 5.5 gives a summary of the specific surface area of some fillers.

Table 5.5. Specific surface area of some fillers

Specific surface area range, m^2/g	**Filler** (the range of specific surface area for the filler is given in parentheses)
0-0.49	aluminum oxide (0.3-1), aluminum trihydroxide (0.1-12), aramid fibers (0.2), barium sulfate (0.4-31), carbon fibers (0.2-1), ceramic beads (0.1-1), glass beads (0.4-0.8), gold powder and flakes (0.05-0.8), pumice (0.4-0.6), sand (0.3-6), silver powder and flakes (0.15-6), wollastonite (0.4-5)
0.5-0.99	bentonite (0.8-1.8), boron nitride (0.5-25), cristobalite (0.4-7), diatomaceous earth (0.7-180), feldspar (0.8-4), nickel powder and flake (0.6-0.7), fused silica (0.8-3.5)
1-4.99	aluminum borate whisker (2.5), antimony trioxide (2-13), barium titanate (2.4-8.5), calcium hydroxide (1-6), lithopone (3-5), magnesium hydroxide (1-30), talc (2.6-35), cellulose fibers (1)
5-9.99	aluminum powder and flakes (5-35), calcium carbonate (5-24), graphite (6-20), kaolin (8-65), titanium dioxide (7-162), zinc sulfide (8)
10-49.99	clay (18-30), nanosize iron oxide (30-60), precipitated silica (12-800), silica gel (40-850), thermal and lamp carbon blacks (10-30), zinc oxide (10-45)
50-99.99	acetylene carbon blacks (65-80), furnace carbon black (50-1475), fumed silica (50-400)
above 100	activated alumina (220-325), attapulgite (120-400), ferrites (210-6000), hydrous calcium silicate (100-180), sepiolite (240-310)

Larger, non-porous particles, such as metals, particles fused by heat, glass spheres, have the lowest specific surface areas. These are followed by mineral particles especially from minerals which cleave to the smooth surfaces of crystals. Fillers which have small particles but are not very porous occupy the middle range of specific surface area. Very small particles, formation of aggregates, and minerals of high porosity give fillers having the highest specific surface areas.

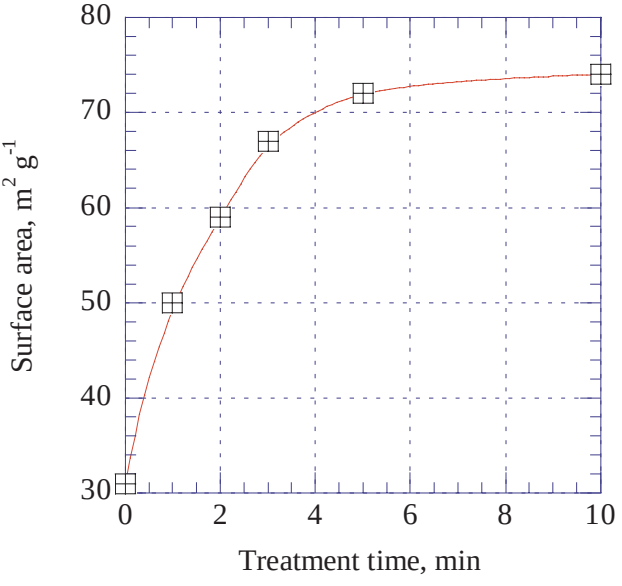

Figure 5.12. Specific surface area of carbon fibers vs. treatment time in oxygen plasma. [Adapted, by permission, from Byung Suk Jin, Kwang Hee Lee, Chul Rim Choe, *Polym. Int*., **34**, No.2, 1994, 181-5.]

From this short analysis, it is evident that specific surface area comprises the total surface of particles including its pores and includes at least part of the free volume in aggregates. For non-porous particles it is useful for calculation of the average particle size. It is also used to calculate the average particle size of materials (such as for example carbon black) which are porous but for which particle size cannot be more precisely determined because of the effect of its structure.

Specific surface area, related to the particle size is a very important parameter. As with particle size, it is useful in helping us to understand how the properties of filled materials are so strongly influenced by fillers.

The specific surface area depends on filler treatment. The treatment of carbon based materials is one of such examples (Figure 5.12).[72] Surface oxidation increases the specific surface area of carbon fibers.

5.7 POROSITY[24,39,69,81-87]

The two extreme cases are zeolite (the smallest pore size) and diatomaceous earth (the largest volume of pores). Zeolites are manufactured with predesigned pore sizes to match the sizes of molecules which can fit into these pores and become absorbed into the pore area. Applications for zeolites include moisture scavenging and selective absorption of various chemical components of mixtures. Diatomaceous earth at the other end of the scale is not selective at all. The large number of pores allows it to absorb 190-600% of its own mass. Applications include absorption of liquids and regulation of rheological properties. The mechanism of rheological control is simple. When the liquid and diatomaceous earth is

mixed and left to stand, the liquid flows into the pores and the viscosity of mixture increases. But when it is mixed again the liquid flows out of the pores and the viscosity drops.

Table 5.6. Pore volume and size of some fillers

Filler	**Pore volume**, cm^3/g	**Pore diameter**, nm
Aluminum oxide		5.8-24
Aluminum oxide[82]		5.8
Calcite[24]	0.0026-0.0136	
Calcium carbonate (ultrafine)[84]	0.1-0.8 (increasing with particle size decreasing)	
Carbon fiber	0.058	0.02-0.05
Carbon fiber[87]		0.017-0.052
Diatomaceous earth	85% of total particle volume	
Microporous polypropylene fibers[83]		230
Precipitated silica[39]	0.2-0.45	2-60 (aggregates)
Precipitated silica[69]	0.1-4.2	7.4-152
Quartz[24]	0.0193-0.0676	
Sepiolite	9.4	
Silica gel		5-40
Zeolites		0.3-1

Many effects can be produced by the pores in filler particles. One is that pores in silica reinforce rubber.[39] During mixing, rubber chains migrate into the pores which increase the adhesion between the phases. The selective absorption of low molecular weight components affects the performance of paints and other materials. Microporous membranes and fibers are produced to clean water and selectively absorb certain solutes.

5.8 PARTICLE-PARTICLE INTERACTION AND SPACING[36,70,71,88-90]

Figure 5.13 shows the potential energy between two neighboring particles. The London-van der Waals forces are attractive and Coulombic forces are repulsive. Their relative magnitudes determine if particles are attracted by each other or repelled. Two methods can be used to overcome the barrier if there is a need to form an agglomeration of particles. One is to reduce distance by using shear forces (mixing) which force particles to come into contact by overcoming the barrier of repulsion. The second method is to increase the ionic concentration which increases attractive forces. Figure 5.14 shows the effect of both methods. The results indicate

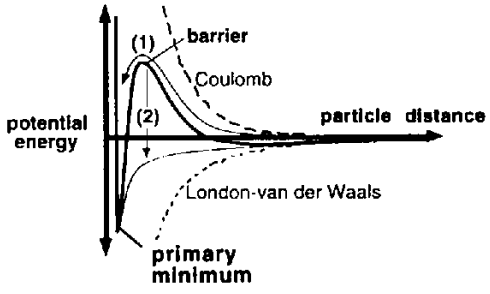

Figure 5.13. Potential energy curve for two colloidal particles. [Adapted, by permission, from Schueler R, Petermann J, Schulte K, Wentzel H P, *Macromol. Symp.,* **104**, 1996, 261-8.]

that by increasing ionic concentration with copper chloride, the contact between particles causes a decrease in resistivity at a lower concentration of carbon black than was possible by applying shear.

Some fillers have a natural tendency to agglomerate (or flocculate) as can be seen from Figure 5.15. Clay particles have a different charge on their crystal face from their crystal edge. Depending on pH these particles are either in a deflocculated state (alkaline environment) or flocculated state (acid environment) as shown in Figure 5.15.

These effects are exploited in commercial applications. In one, conductive particles are expected to come to close contact with each other in conductive plastics. In another, the flocculated state is required in regulating rheological properties of coatings. But in many other cases, the opposite effect is required – the filler is incorporated to form a homogeneous well dispersed mixture.

The two terms: agglomeration and flocculation require some clarification. Agglomeration is defined as a gathering of smaller particles into larger size units.

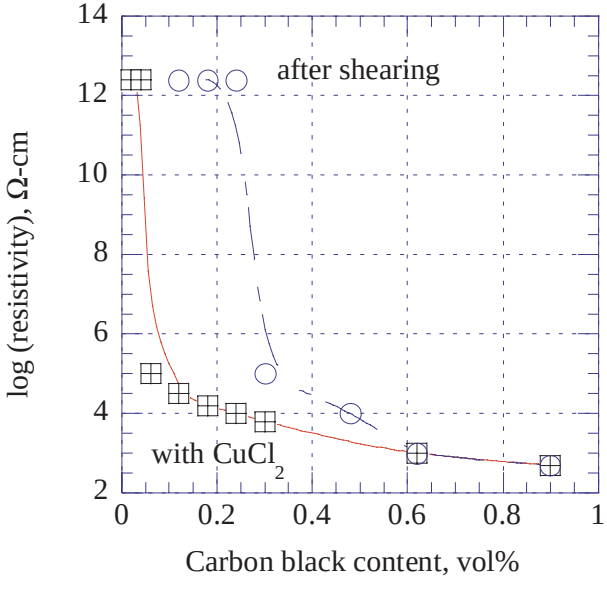

Figure 5.14. Resistivity of epoxy resin vs. carbon black concentration. [Data from Schueler R, Petermann J, Schulte K, Wentzel H P, *Macromol. Symp.,* **104**, 1996, 261-8.]

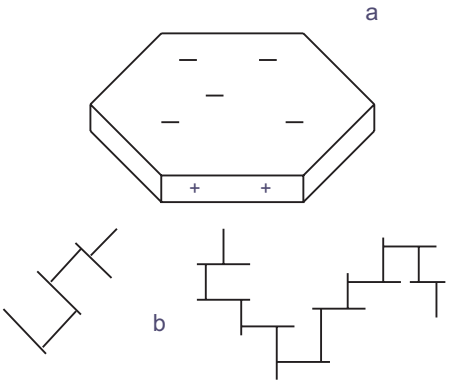

Figure 5.15. Positive and negative charges on clay particles (a). Flocculated state (b).

This phenomenon occurs in fillers during storage. As the storage time gets longer, the agglomeration of particles increases to the extent that stored filler requires substantially higher dispersion forces than does freshly manufactured filler. The mechanical forces to which the filler is exposed during transportation and the compaction that occurs as a result of storing several layers of bags or layers of filler in silo increase agglomeration. The word agglomeration is used to describe changes in the particulate materials in their solid state. Many industrial compaction methods are based on agglomeration. Flocculation is a similar process but usually occurs in a liquid medium. The name is derived from the word "flock" which describes the appearance of flocculated particles. The flocculation process is often associated with the coagulation of particles in water treatment with flocculants. It is also occurs in paints but this is usually undesirable. More information on this subject is included in the separate sections below.

The mean particle spacing can be calculated using the following equation:

$$s = (k\phi^{-1/3} - 1)d \qquad [5.5]$$

where:

s	interparticle spacing
d	particle diameter
ϕ	volume fraction

In this equation, the coefficient k depends on particle arrangement. For face-centered particles in their closest arrangement, the value for k is 0.906.

5.9 AGGLOMERATES[3,29,39,77,89,91-95]

Both agglomeration and flocculation lead to a similar result, in the sense that two or more particles join together to form a bigger one. Filler particles are mostly composed of primary particles but some are pre-formed aggregates (carbon blacks). Agglomeration and flocculation adversely affects the dispersion stability of fillers. But there are many technological advantages of agglomeration.

Van der Waals forces are primarily responsible for agglomeration of fillers during production and storage. These forces are especially important during the dispersion of fillers. For agglomeration to occur the sum of all environmental forces

(gravity, inertia, drag, etc.) must be smaller than the forces between the adhering partners:

$$T_a = \frac{\sum_i B_i}{\sum_j E_j} > 1 \qquad [5.5]$$

where:

T_a	tendency to adhere
B_i	binding forces
E_j	environmental forces

This equation shows the forces that cause agglomeration and deagglomeration. The forces causing adhesion between particles can be grouped as follows:

- **Bridging**: sintering, melting, the effect binders, chemical reaction
- **Adhesion and cohesion**: the effect of viscous binders and adsorption layers
- **Attraction forces**: van der Waals, hydrogen bonding, electrostatic and magnetic
- **Interfacial forces**: liquid bridges (H_2O – hydrogen bonding), capillary.

The agglomeration forces can be measured by determining the tensile strength of compacted fillers. Tensile strength depends on the packing density and the type of filler. Tensile strength and, therefore, agglomeration also depends on the type of mechanical processes used for filler dispersion. Pelletized carbon black does not return to its former agglomeration after grinding, and the intensity of grinding determines the resultant packing density and the tensile strength. Organic treatment of the titanium dioxide surface may decrease agglomeration as manifested by a lower tensile strength of similarly compacted material at the same packing densities. Agglomeration of titanium dioxide particles has been found to be due to water adsorption through liquid bridging, rather than by van der Waals forces, which usually prevail with carbon blacks.

Agglomeration has an effect on fillers used in various industrial processes. Dispersion of carbon black, especially that having very fine particles, is difficult. On the other hand, the agglomeration process is broadly used in the pharmaceutical industry to pelletize various ingredients where the mechanical strength of pellets is important. It is well-known that carbon black is not composed of individual primary particles but of primary particles joined together into aggregates. Even a prolonged effort to grind materials containing carbon black does not result in a change of their aggregates' size. Forces holding individual particles together are sufficiently strong to resist even very intensive grinding or mixing. Other agglomeration processes are based on the formation of hydrogen bonds. Individual particles such as fumed silica form networks of aggregates.

From the above discussion, one can see that agglomeration, depending on the type of mechanism, leads to formation of aggregates which can be weakly bonded or have very strong bonds, resisting even extensive grinding. Apart from the

mechanism of bonding and type of bonding forces utilized, the differences in agglomeration are related to particle size, type of surface, chemical groups available on the surface, moisture level, effect of surface treatment, method of filler production, etc. Agglomeration processes are complex in nature and, if they are to be either prevented or enhanced, the nature of agglomeration must be carefully studied.

Several processes benefit from agglomeration. They include: wet mixing, suspending, rheological modification, drying, fluidized-bed processes, clarification, briquetting, tableting, pelletizing, and sintering. Processes negatively affected by agglomeration include: dispersion, dry grinding, screening, dry mixing, conveying, silos storage, etc.

5.10 AGGREGATES AND STRUCTURE[23,39,50,52,56,62,70,91,96-107]

Aggregates and structure are very important morphological features of carbon black and to a lesser extent of silica fillers. The aggregate of carbon black is a cluster of primary particles which are fused together and can be separated only by extensive mechanical forces which seldom exist in typical mixing operations. The aggregates of silica are formed by chemical and physical-chemical interactions which cause the formation of an assembly of particles which are the smallest units not subdivided by mixing.[39] The aggregate can be quantified by the size of the primary particles, the number of primary particles in the aggregate, and their geometrical arrangement in the aggregate. The term "structure" encompasses all these three parameters to give a general measure of the aggregate. A low structure carbon black contains less particles and limited branching. It is perceived as spherical assemblage of particles. A high structure carbon black is represented more by a grape-like structure with numerous branches.

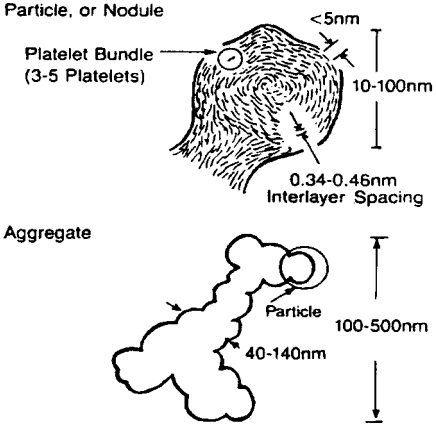

Figure 5.16. Structure of carbon black primary particle and aggregate. [Adapted, by permission, from Byers J T, Meeting of the Rubber Division, ACS, Cleveland, October 17-20, 1995, paper B.]

Figure 5.16 gives a schematic diagram which compares various dimensions in carbon black particles and aggregates. Compared with the small dimensions of voids within particle and the particle itself, the aggregate is a fairly large object of irregular morphological structure. As much as the application of carbon black is related to its morphology, its structure relates to vehicle (or binder) demand.

Scientists are continuing to make a major effort to determine the structure of carbon black and to apply this knowledge to its manufacture and application.

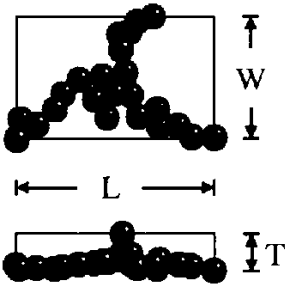

Figure 5.17. Two views of N220 aggregate model obtained by 90° rotation. [Adapted, by permission, from Gruber T C, Zerda T W, Gerspacher M, *Rubb. Chem. Technol*., **67**, No.2, 1994, 280-7.]

Several methods are used including oil absorption, transmission electron microscopy, compression, and thermoporometry. The analytical results must be further analyzed by various algorithms to transform the results to a form which can be used for the prediction of properties of the compounded materials. Various forms of microscopy are applied in research studies and the findings have contributed to the further understanding of this complex subject. Figure 5.17 illustrates the essential problem related to microscopy. Because of the very small size of primary particles, only TEM gives sufficient resolution to elucidate morphological features. But, TEM can produce only two dimensional micrographs which do not display the spatial distribution of primary particles in the aggregate. In addition, the image projected depends on the viewing angle. Figure 5.17 shows the same aggregate displayed from angular views which differ by 90°.[96] The aim of this study[96] was to develop a technique for three dimensional analysis of carbon black aggregates. The results indicate that tread-grades of carbon black are planar and highly branched similar to the aggregates displayed in Figure 5.17.

High surface area carbon black was studied using small angle neutron scattering and contrast variation. It was found that aggregates are built out of 4-6 primary particles which can be represented by a prolate ellipsoid with semi-axes at 14.5 and 76.4 nm. This method can determine the average number of particles forming the aggregate.

In the case of carbon black, the aggregates are distributed in the matrix rather than individual particles, it is therefore important in some applications (e.g., conductive plastics) to evaluate the distance between these aggregates. It is now possible to measure these distances by atomic force microscopy coupled with straining device.[106] There is a linear relationship between the parallel distance between aggregates dispersed in SBR and strain value. For 10 phr of N 234, the mean distance between aggregates varied in a range from 1.85 to 3.42 μm. For practical purposes, a modified equation [5.4] is used to determine the interaggregate distance:

$$s = [k(\beta\phi)^{-1/3} - 1]d_{St} \qquad [5.6]$$

where:

s	interparticle spacing
k	coefficient of spatial arrangement
β	$=1 + (0.7325 \times \text{DBPA} - 15.75) \times 10^{-2}$, Medalia's coefficient based on DBP absorption
d_{St}	Stokes particle diameter
ϕ	volume fraction

This is a complex area of investigations and far from being complete. Until mathematical criteria characterizing the structure are developed, the available quality control and research data is the only source of information that can be used to select carbon black for specific application.

5.11 FLOCCULATION AND SEDIMENTATION[89,108-112]

Flocculation of pigment is a mechanism exploited to facilitate a higher retention of pigment in the paper manufacture. Heteroflocculation is induced by the addition of cationic polyacrylamide to the pulp and clay mixture. The retention of clay is dramatically improved and clay distribution becomes more even. This is an example of how a controlled flocculation process may help to achieve certain technological goals. In paint production, too, the addition of flocculants not only inhibits phase separation but also allows the reversal of separation by preventing sediment compaction. On the other hand, a good dispersion of pigment can be completely reversed by the addition of auxiliary agents which eliminate particle charge (decreasing ζ-potentials – for more information see separate section below). Such an addition affects not only the durability of the product but also its brightness, color, and opacity. Flocculation also depends on the pigment concentration. The higher the flocculation gradient, the more the pigment flocculates.

Figure 5.18 shows a schematic representation of montmorillonite particles in dispersions. This diagram helps us to distinguish between different types of flocculation. Figure 5.18a depicts internal mutual flocculation which is described in Figure 5.15. As a result of electrostatic and van der Waals forces between the edges and faces of particles, a house-of-cards structure is formed (the pH of the dispersion or its ionic strength influence this effect). Under shearing conditions, the orientation of particles changes (5.18b) which affects viscosity. Figure 5.18c shows face-to-face flocculation or heteroflocculation. Heteroflocculation requires a second component such as polyvalent cation used in paper manufacturing. The polyvalent cation reverses the surface charge and changes the electrokinetic potential, resulting in the collapse of a voluminous gel structure into compact face-to-face packing.[108]

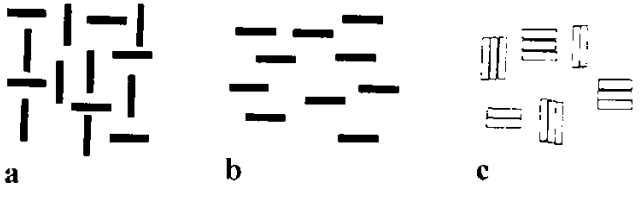

Figure 5.18, A schematic representation of montmorillonite particles in dispersion. [Adapted, by permission, from Miano F, Rabaioli M R, *Coll. & Surfaces*, **84**, Nos.2/3, 1994, 229-37.]

Flocculation affects filler packing and therefore it also affects surface roughness and gloss. The composition of fillers (pigments) can be changed by co-flocculation. Special additives are used to promote this effect because co-

flocculation is seen as one of the mechanisms which can be used to overcome flooding and floating. Co-flocculating agents, by bridging two different particles, restrict their movement which contributes to a better color development in the material or a more uniform composition in the case of filled material. Excessive co-flocculation detracts from gloss and changes rheological properties.

The rheology of the suspension is affected through the particle interaction coefficient:

$$\sigma = \sigma_S + \sigma_P \qquad [5.7]$$

where

σ_S	contribution of solvent, flocculating agents, etc.
σ_P =	σ_{PC} / D_1, summation of all individual particle contributions to the particle interaction coefficient
σ_{PC}	particle contribution constant
D_1	number average particle size

This equation has been confirmed by experimental results.[109] These have shown that the interaction parameter increases as the particle size decreases. The particle interaction coefficient, σ, in the following equation is required to describe the viscosity-concentration relationship of suspensions:

$$\ln\frac{\eta}{\eta_0} = \frac{[\eta]\varphi_n}{\sigma - 1}\left[\left(\frac{\varphi_n - \varphi}{\varphi_n}\right)^{1-\sigma} - 1\right] \qquad [5.8]$$

where

σ	particle interaction coefficient
η	suspension viscosity
η_0	suspending medium viscosity
$[\eta]$	intrinsic viscosity
φ_n	particle packing fraction
φ	suspension particle volume concentration

Filler particles can be modified to decrease flocculation. Kaolin particles modified by a graft of poly(ethylene oxide) showed an increase in the upper critical flocculation temperature. Stabilization of particle dispersion was due to an enhanced steric stabilization.[112]

In rubber systems containing carbon black, flocculation may cause substantial changes in mechanical properties. Flocculation in these systems counteracts filler dispersion. Carbon black flocculation occurs in filled rubber stock during storage or during vulcanization in the absence of shear.[111] Temperature is the important kinetic factor which affects the flocculation rate (Figure 5.19). In addition to temperature and time, flocculation depends on the type of carbon black and its concentration.

Sedimentation occurs readily in suspensions in low viscosity liquids. The sedimentation coefficient is given by the equation:

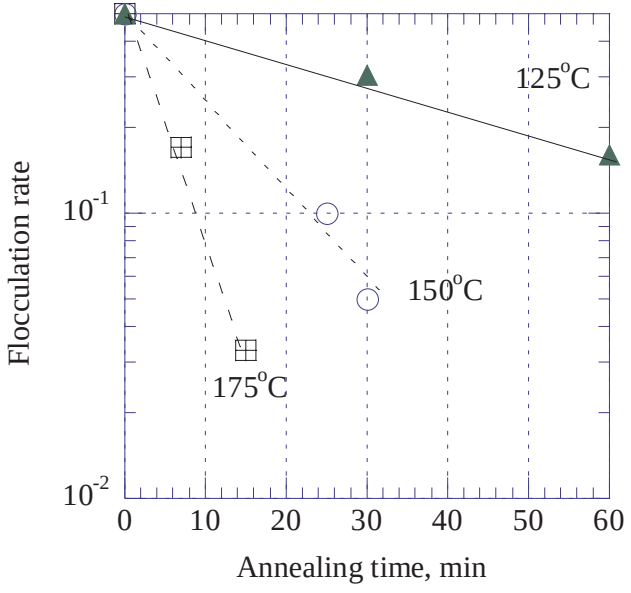

Figure 5.19. Rate of carbon black flocculation at different temperatures. [Adapted, by permission, from Boehm G G A, Nguyen M N, *J. Appl. Polym. Sci.*, **55**, No.7, 1995, 1041-50.]

$$s_0 = \frac{4/3\pi R^3(\rho_f - \rho_p)}{6\pi\eta_0 R} \qquad [5.9]$$

where

R	particle radius
ρ_f	density of the fluid
ρ_p	density of a particle
η_0	viscosity of fluid medium

Since particles absorb components of the system to form adlayers (or bound polymer layers) the radius of the particle has to be corrected as follows:[110]

$$R_e = R + \Delta r = \frac{(\phi V \rho_f)^{1/3}}{W} \qquad [5.10]$$

where

R_e	effective radius of particle
Δr	thickness of adlayer
ϕ	packing factor
V	bulk sediment volume
W	weight of particles

5.12 ASPECT RATIO[113-117]

Aspect ratio is the length of a particle divided by its diameter. Table 5.7 provides information on aspect ratios of some fillers.

Table 5.7. Aspect ratio of some fillers

Aspect ratio range	**Filler** (actual aspect ratios are given in parentheses)
1-3	ferrites (1-5); majority of particulate fillers
3-10	milled carbon fiber (6-30), milled glass fiber (3-25), talc (5-20), wollastonite (4-68)
10-20	silver-coated nickel flakes (15), nickel flakes (15-50)
20-100	aluminum flakes (20-100), mica (10-70)
above 100	aramid fibers (100-500), chopped carbon fibers (860), chopped glass fibers (250-800), hollow graphite fibrils (100-1000), nickel-coated carbon fibers (200-1600)

The majority of fillers fall into a group of low aspect ratio fillers (below 10). Reinforcing elongated particles of mineral origin have an aspect ratio between 10 and 70. Fibers (except for milled fibers) have aspect ratios well above 100. The aspect ratio of fibers is a critical parameter in composites[115,117] and in providing electrical and shielding properties.[116] For reinforcement, high aspect ratios are more effective. Also, in electrical applications high aspect ratio fillers give good performance at substantially lower concentrations and a typical aspect ratio is in a range from 20 to 100. The initial aspect ratio of filler is not necessarily retained in the final product because of degradation of fiber length during processing.

5.13 PACKING VOLUME[1,3,9,17,20,90,109,113,118-128]

The maximum packing volume of a filler can be calculated for different geometrical arrangements, determined after the filler is dispersed in a liquid media (e.g. oil). It is calculated by dividing the tamped bulk density by specific gravity of filler. Table 5.8 compares the data obtained from calculation for monodispersed spheres in different arrangements with determined values.

The data in the Table 5.8 show that a high packing volume can be obtained in real systems as compared with theoretical calculation results. A particle size decrease results in a decrease in the maximum volume packing fraction. A surface coating can increase the maximum volume packing fraction by reducing the thickness of the bound polymer. The above data shows that a higher packing was obtained in experimental systems than was predicted for monodispersed spheres. This is a result of the mixture of particle sizes which fill voids more efficiently.

In polymeric systems, particle size has to be corrected for the thickness of the occluded polymer layer. This can be done by the use of the volume coefficient of separation, α, given by the following equation:

$$\alpha = (1 + h / d)^3 \qquad [5.11]$$

where
h the thickness of the matrix interlayer
d particle diameter

Table 5.8. Maximum packing volume calculated for monodispersed spheres and determined for some fillers[9,90]

Spatial configuration or fillers in different media	Maximum packing volume fraction
Theoretical calculations	
Hexagonal or pyramidal arrangement (maximum packing)	0.74
Double staggered layout	0.70
Random close packing	0.64
Random loose packing (simple staggered)	0.60
Cubic	0.52
Experimental results	
Glass beads in polyethylene	0.68
Ground calcium carbonate (10 μm) in polyethylene	0.52
Precipitated calcium carbonate (2 μm) in polyethylene	0.44
Ground calcium carbonate (1 μm) in mineral oil	0.55
Ground calcium carbonate (3 μm) in mineral oil	0.59
Precipitated calcium carbonate (0.6 μm) in mineral oil	0.30
Surface treated ground calcium carbonate (1 μm) in mineral oil	0.77
Surface treated ground calcium carbonate (3 μm) in mineral oil	0.76

The maximum volume packing fraction can also be estimated but with much lower precision by dividing bulk density by specific density. The lower precision results from the fact that particle packing depends on an arrangement of loosely packed particles which is not ideal for measuring bulk density. Table 5.9 gives data calculated for a large number of grades of different fillers using this method. Tamped density was taken as the bulk density which gives more realistic values.

The values in Table 5.9 are far from the theoretical values presented in the Table 5.8. Only a few fillers included in the last row come close to the values from theoretical calculations. In most cases, fillers are manufactured to offer a broad range of packing densities so that one can be selected according to the requirements which may not always be maximum packing. The information on maximum packing volume is important to realize cost savings and to maximize mechanical properties. If cost savings is an important consideration then the filler or fillers combination which offer the most efficient packing and thus the highest level of filler incorporation should be selected. Otherwise, maximum packing density and a correction for bound polymer should be always evaluated to ensure that fillers are not used in excessive amounts. Mechanical properties decrease rapidly as maximum volume packing is approached.

Table 5.9. Maximum packing volume fraction, ϕ_M, of some fillers calculated by dividing tamped density by specific density of filler

ϕ_M **range**	**Filler** (the range of ϕ_M for a given filler is given in parentheses)
0.01-0.099	aluminum flakes (0.07-0.17), fumed silica (0.02-0.06), graphite (0.09-0.46), milled glass fiber (0.07-0.43), nickel powder (0.9-0.33)
0.1-0.19	calcium carbonate (0.18-0.53), carbon black (0.15-0.28), kaolin (0.11-0.34), PTFE powder (0.12-0.15), talc (0.16-0.42), silver flake (0.17-0.4), silver powder (0.13-0.52), silver spheres (0.1-0.48), titanium dioxide (0.19-0.3), wollastonite (0.13-0.47), zinc sulfide (0.17-0.23)
0.2-0.29	aluminum trihydroxide (0.2-0.55), chopped glass fiber (0.21-0.28), cristobalite (0.26-0.36), gold spheres (0.21-0.48), mica (0.22-0.42)
0.3-0.39	barite (0.35-0.50)
above 0.4	aluminum needles and tadpoles (0.47-0.6), hollow glass beads (0.53-0.66), polymeric beads (0.4), silica flour (0.5-0.65), stainless steel powder (0.63)

Packing density must be understood when lowering the viscosity of system, increasing thermal conductivity and heat dissipation, increasing electric conductivity, designing electronic devices which are protected from overloading, designing materials of high and low specific densities, etc.

The data in Figure 5.20 demonstrates another aspect of packing density. Nanoparticle size Al_2O_3 was slurried in water and compressed in a die. The results show that the density of pellet is very close to the specific density of the material if sufficient pressure is applied. In real applications, high pressures result from various forces operating in the system such as equipment conditions, crystallization, shrinkage, and chemical bonding. All these factors influence the potential maximum loading in a real systems.

Three factors associated with particle packing are common use: critical volume fraction (or loading), effective volume fraction, and critical pigment volume concentration. The effective volume fraction of a filler includes the filler and the elastomer immobilized within the aggregates. This is given by the equation:[3]

$$\phi_e = (\phi_a \times \alpha) + \phi_t \qquad [5.12]$$

where

ϕ_a volume fraction of agglomerates
α volume fraction of immobilized rubber
ϕ_t volume fraction of carbon black

The coefficient α which corrects for the incorporated polymer layer in a manner similar to equation [5.11] is obtained for carbon black from the oil absorption and calculated from the equation:

$$\alpha = DBPA / [DBPA + (100 / \rho)] \qquad [5.13]$$

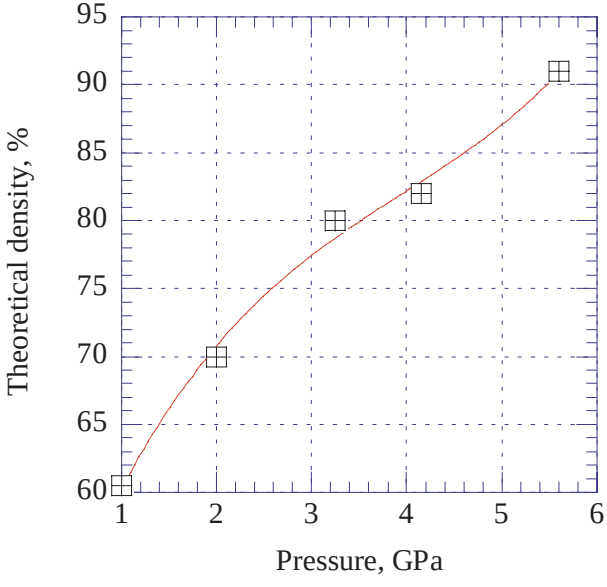

Figure 5.20. Density of Al_2O_3 samples vs. compression pressure. [Adapted, by permission, from Gallas M R, Rosa A R, Costa T H, da Jornada J A H, *J. Mater. Res.,* **12**, No. 3, 1997, 764-8.]

where
DBPA dibutyl phthalate absorption
ρ carbon black density

The critical volume fraction of filler is the volume of filler above which a property change occurs or above which the rate of change of that property is increased. Figure 5.21 illustrates the meaning of this critical value in the studies of carbon black flocculation. The critical volume fraction of N347 carbon black used in this study is at 13 vol%. At 20 phr (10 vol%), there is no change in the excess storage modulus because the carbon black aggregates are too far apart and unable to migrate far enough to flocculate. At 30 phr (14 vol%), the composition is just above the critical volume fraction of filler and small changes occur. If still more carbon black is added (50 phr) flocculation occurs rapidly.

Figure 5.22 shows that the critical filler volume fraction depends on the structure of carbon black which is here characterized by DBP absorption.

The critical volume fraction of the filler has a different application in the case of conductive materials. As the amount of conductive filler is increased, the material reaches a percolation threshold. Below the percolation threshold concentration, the electric conductivity is similar to that of matrix. Above the percolation threshold conductivity rapidly increases. Above the critical volume fraction of filler which is, in turn, a concentration above the percolation threshold, there is a rapid increase in conductivity.[94] The critical volume fraction depends on the type of filler and its particles size. For example, for silver powder, it ranges from 5 to 20 vol% for

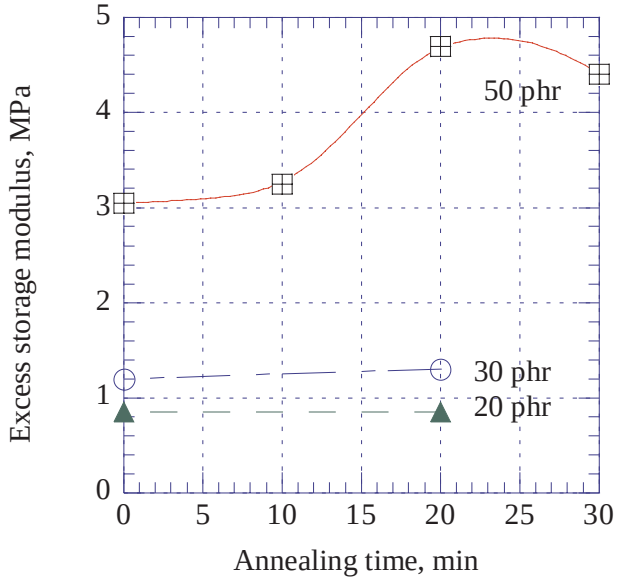

Figure 5.21. Excess storage modulus of carbon black filled polybutadiene vs. annealing time. [Adapted, by permission, from Boehm G G A, Nguyen M N, *J. Appl. Polym. Sci.*, **55**, No.7, 1995, 1041-50.]

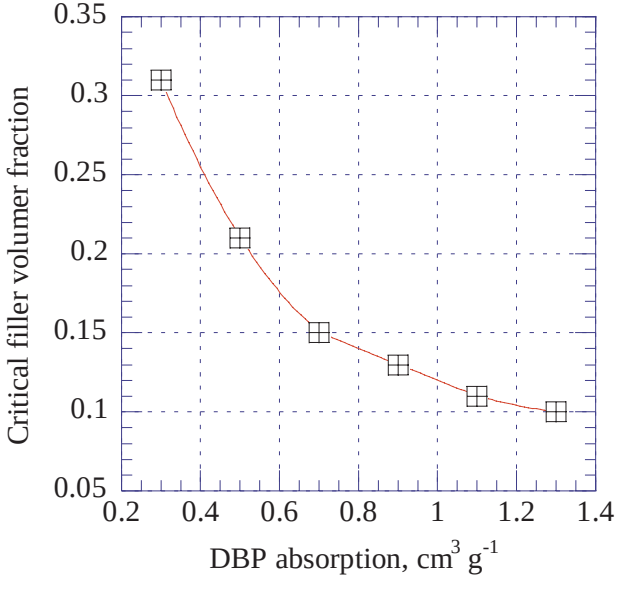

Figure 5.22. Critical volume fraction of carbon black vs. DBP absorption. [Adapted, by permission, from Boehm G G A, Nguyen M N, *J. Appl. Polym. Sci.*, **55**, No.7, 1995, 1041-50.]

particle sizes in the range of 0.5 to 9 μm (the smaller the particles size the smaller the critical volume fraction).

The concept of critical pigment volume concentration was introduced about 50 years ago by Asbeck and van Loo to explain the sudden change in paint properties around a certain concentration of pigment. Above this concentration, gloss rapidly decreases, porosity and water permeability increases, and the film becomes brittle. This is caused by the fact that there is not enough binder to fill the voids between particles and encapsulate them. Solvent-based paints are usually formulated well below the critical pigment concentration. The critical pigment concentration is calculated from the equation:[128]

$$CPVC = \frac{V_{pigment} + V_{filler}}{V_{pigment} + V_{filler} + bV_{vehicle}} \qquad [5.14]$$

where

$V_{pigment}$ volume of pigment
V_{filler} volume of filler
$V_{vehicle}$ volume of resin
b constant, b = 1 for solvent paints and b > 1 for latex paints

5.14 pH[129-130]

Table 5.10 pH of filler slurry

pH range	**Filler** (the range of pH for a filler is given in parentheses)
1-2.9	antimony pentoxide (2.5-9), antimony trioxide (2-6.5), carbon black (2-8)
3-4.9	ceramic beads (4-8), cellulose fibers (4-9), clay (3.9-9), kaolin (3.5-11) fumed silica - hydrophilic (3.6-4.5), fumed silica - hydrophobic (3.5-11), precipitated silica (3.5-9), titanium dioxide (3.5-10.5)
5-6.9	attapulgite (6.5-9.5), barium sulfate (6-9.5), calcium sulfate (6.8-10.8), diatomaceous earth (6.5-10), glass fibers (5-10), muscovite mica (6.5-8.5), perlite (5.5-8.5), quartz (6-7.8), sand (6.8-7.2), silica gel (6.5-7.5), slate flour (6.5-8.1), wood flour (5), zinc sulfide (6-7)
7-8.9	aluminum oxide (8-10), aluminum trihydroxide (8-10.5), anthracite (7-7.5), barium and strontium sulfate (7-7.5), bentonite (7-10.6), cristobalite (8.5), feldspar (8.2-9.3), glass beads (7-9.4), hydrous calcium silicate (8.4-9), iron oxide (7-9), lithopone (7-8), phlogopite mica (7-8.5), sepiolite (7.5-8.5), talc (8.7-10.6), vermiculite (7), zinc borate (8.1-8.3)
9-10.9	barium metaborate (9.8-10.3), calcium carbonate (9-9.5), fused silica (9), wollastonite (9.8-10), zeolites (10-12), zinc stannate (9-10)
11 and above	calcium hydroxide (11.4-12.6)

The majority of fillers have a pH close to neutral. But many fillers have a broad range of pH which is either due to their origin, manufacturing technology, or surface treatment. The pH of filler may strongly affect interaction with other components of the mixture, so it is possible to chose fillers for specific application. While this gives additional methods of influencing properties of materials, it requires care in selecting an appropriate filler.

Fillers can be degraded either by too high or too low a pH[130] or modified by polymer conformation. The modifications causes a change in the surface coating of the filler.[129]

5.15 ζ-POTENTIAL[108,131-134]

The electric charge distribution in the plane of shear (or in the plane perpendicular to the surface) is referred to as ζ-potential (zeta-potential). The surface charges on the pigment or filler particles are formed as a result of dissociation of functional surface groups or adsorption of countercharges from the liquid phase. The development of surface charge on the particle is accompanied by the formation of countercharge in the surrounding medium which results in the electrochemical double layer. This double layer plays an essential role in stabilization of colloids and suspensions. Stabilization occurs when the liquid phase has a high dielectric constant, thus the stabilization effect is more pronounced in water rather than in solvent media.

The ζ-potential depends on the pH of the liquid phase. The pH at which the ζ-potential is zero is called the isoelectric point. The isoelectric point of each filler depends on its surface structure. In the case of titanium dioxide, the isoelectric point depends on the surface coating. A SiO_2 coating decreases the isoelectric point whereas Al_2O_3 increases it.[134]

Also electrolytes and polyelectrolytes affect the ζ-potential. Studies on montmorillonite clays showed that an excess of Na^+ ions in solution does not produce changes in ζ-potential although it is known that Na^+ ions react with the edges of clay. Thus, only interaction with the face of crystal affects ζ-potential. Ca^{2+} ions can replace sodium counterions on the montmorillonite face and this replacement causes a shift towards negative values of ζ-potential. When Ca^{2+} ions replace sodium counterions on the montmorillonite face they cause deflocculation and an increase in viscosity.[108]

The measurement of ζ-potential was used to control the flotation recovery of kaolin and calcium carbonate from waste paper.[131] The addition of a cationic polymer changes its usually negative values of ζ-potential of kaolin and calcium carbonate (-60 and -40 mV, respectively). The ζ-potential becomes positive when the concentration of polyelectrolyte reaches 5×10^{-4} g/l then gradually increases until a plateau is reached at about 1×10^{-3} g/l. The final ζ-potential is higher for kaolin than calcium carbonate. This interaction with the polyelectrolyte results in large particles which are more readily separated and recovered.[131]

The ζ-potential of colloidal silica surface treated by acrylate copolymers is affected by pH. The ζ-potential of untreated colloidal silica at a pH of 4 is -7 mV and it decreases to -32 mV at a pH of 7.[132] Modification of the surface of colloidal silica changes its surface properties and behavior. In another study on filler modification,[133] hydroxyapatite was modified for medical applications with several differ-

ent silanes. The ζ-potential depended to a large extent on silane composition and the pH of surrounding liquid.

5.16 SURFACE ENERGY[6,20,23,66,72,74,84,90,104,112,135-159]

The following subjects, which are related to surface energy, are included in this discussion: wettability, acid-base interaction, and work of adhesion. The interrelation is well illustrated by the set of equations.

Particles in a matrix are either spontaneously wetted or remain unwetted by polymer depending on the relative magnitudes of their solid/vapor surface energy, γ_{SV}, and liquid/vapor surface energy, γ_{LV}. The following equations may be used to calculate these energies:[90]

equation of state

$$\cos\theta = 1 + b\ln(\gamma_c / \gamma_{LV}) \quad [5.15]$$

solid/vapor surface energy

$$\gamma_{SV} = [b\exp(1/b - 1)]\gamma_c \quad [5.16]$$

liquid/solid surface energy

$$\gamma_{LS} = \gamma_{SV} + \gamma_{LV} - \gamma_{LV}\left[1 + b\exp\left(1 - \frac{1}{b}\right) + b\exp\left(1 - \frac{1}{b}\right)\ln\frac{\gamma_{SV}}{b\gamma_{LV}}\right] \quad [5.17]$$

where

θ	contact angle of filler wetted by a liquid
b	Lee interaction parameter
γ_c	critical surface tension
γ_{LV}	liquid/vapor surface energy
γ_{SV}	solid/vapor surface energy
γ_{LS}	liquid/solid surface energy

Both surface tension energies can be determined from contact angle measurement and $\bar{b}$ can be obtained as a geometrical mean between the b values of the constituents. Plotting the surface energy ratio between filler and polymer vs. extent of interaction, $\bar{b}$, it is possible to obtain the matrix shown in Figure 5.23. The results of similar determinations for any given system can be plotted on this matrix to establish in which zone the actual system resides. The lines separating various zones on the matrix were plotted based on the following relationships:

equilibrium work of adhesion

$$W_{LS} = \gamma_{LV}[b\ln(\gamma_{SV} / \gamma_{LV}) + b + 1 - b\ln b] \quad [5.18]$$

Harkins spreading coefficient

$$\lambda_{LS} = \gamma_{LV} b[\exp(1 - 1/b)]\{1 + \ln[\gamma_{SV} b\gamma_{LV}]\} - 1 \quad [5.19]$$

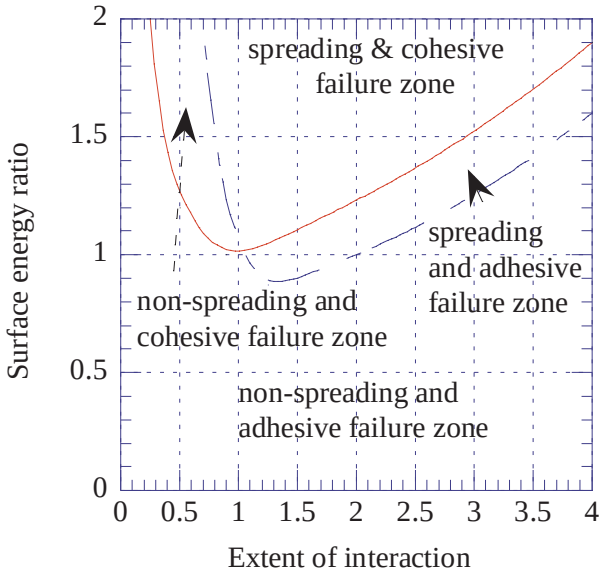

Figure 5.23. Spreading and failure characteristics predicted from the theory of adhesion. [Adapted, by permission, from Bomal Y, Godard P, *Polym. Engng. Sci.*, 36, No.2, 1996, 237-43.]

The method of determination is given elsewhere.[158,159] For our purposes, the above discussion shows that both wetting of fillers and the adhesion between filler and the matrix is governed by the principles of the theory of adhesion based on the surface energy properties of the filler and the matrix.

This method allows one to evaluate an unknown system. The following discussion concentrates on the surface properties of different fillers. The current level of understanding has been developed from principles proposed by Fowkes who indicated that the work of adhesion has two components:

$$W_a = W^d + W^{sp} \qquad [5.20]$$

where

W^d	contribution of dispersive, non-specific or London-type forces
W^{sp}	contribution of specific interactions such as dipole-dipole, H-bonding, acid-base, etc.

Accordingly, the surface free energy of a solid can be expressed as a sum of dispersive and specific components:

$$\gamma_S = \gamma_S^d + \gamma_S^{sp} \qquad [5.21]$$

where

γ_S^d	dispersive component of surface free energy
γ_S^{sp}	specific component of surface free energy

The dispersive component is associated with polymer-filler interaction and the specific component is associated with filler networking and agglomeration. The dispersive component of different fillers is more conveniently measured by inverse gas chromatography although it can also be measured by contact angle methods. The work of adhesion is given by the following equation, which has been modified to account for Fowkes theory,

$$W_a = 2Na[(\gamma_1^d \gamma_2^d)^{0.5} + (\gamma_1^p \gamma_2^p)^{0.5}] \qquad [5.22]$$

where

N	Avogadro number
a	surface area of adsorbed molecule
1,2	subscripts denoting filler and polymer or pigment and liquid
d,p	superscripts denoting dispersive and polar components

The work of adhesion increases as the dispersive component of surface free energy increases. Table 5.11 gives the values of the dispersive component available in the literature for different fillers.

Table 5.11. Dispersive components of different fillers

Filler	$\gamma^{\mathbf{d}}$, mJ/m^2	**Reference**
γ-aluminum oxide	92	136
calcium carbonate (Socal Solvay, Milicarb Omya, Albacar 5970) calcium carbonate precipitated & maleated	52/48/53 64.3 & 32.8	136 139
carbon black (range for numerous grades) carbon black oxidized and unoxidized carbon black	40-120 41.9-43.4 51	23 145 149
carbon fiber treated by plasma in different concentration of CF_4/O_2	17.7-36.9	143
fumed silica	80	136
magnesium oxide	95	136
muscovite mica	70	136
silica silica precipitated (Zeosil 175) silica precipitated (Zeosil 175), esterified with alcohols C_{16}-C_1 silica precipitated (Zeosil 175), methacryl and vinyl silane modified	49.8 105 46-87 84 & 84	20 137 137 137
talc	130	136
titanium dioxide non-coated Al_2O_3 and SiO_2 coated	76 50.3 104.3 & 124.8	136 20 20
zinc oxide	52	136

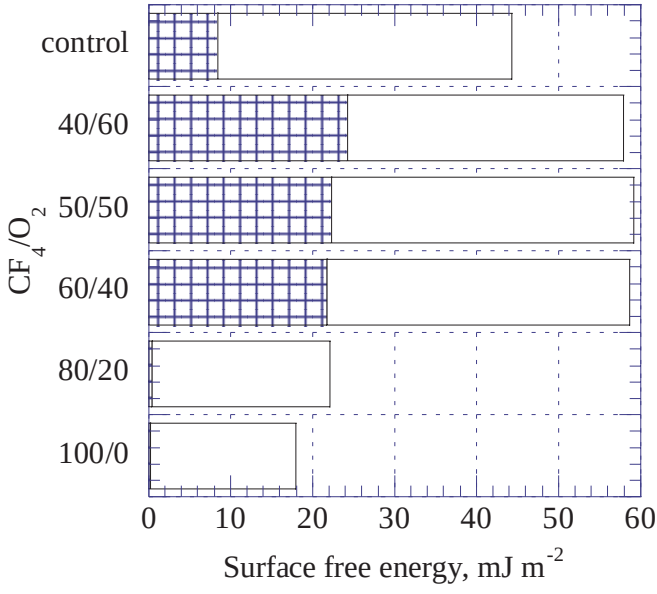

Figure 5.24. Surface energy components of carbon fibers treated with plasma in the presence of different gas composition. Open bars - γ_S^d, shaded bars - γ_S^p. [Data from Tsutsumi K, Ban K, Shibata K, Okazaki S, Kogoma M, *J. Adhesion*, **57**, Nos.1-4, 1996, 45-53.]

Various surface modifying operations such as silane coating, maleation, oxidation, surface coating have a noticeable effect on surface energy.

Figure 5.24 shows the effect of oxidation on dispersive and polar components of surface free energy. Carbon fibers were exposed to plasma treatment in the presence of various ratios of CF_4 and O_2. The untreated sample and the samples exposed to a substantial concentrations of oxygen show increase in the polar component. High concentrations of CF_4 gas reduced its dispersive component and converted the surface to a PTFE-like material as confirmed by XPS studies.[143]

Acid-base interaction which results from polar interaction can be predicted from the inverse gas chromatography data. The basic relationship used in this type of studies is:[148]

$$\Delta H_{ab} = Ka\,DN + Kd\,AN \qquad [5.23]$$

where

ΔH_{ab}	enthalpy of absorption
Ka, Kd	the solids' acid-base interaction parameters
AN DN	literature values of vapors' acid-base interaction

The values of Ka and Kd can be measured from the plots of $\Delta H_{ab}/AN$ vs. DN/AN. The methods of determination and result interpretations are discussed elsewhere.[66,136148,157]

5.17 MOISTURE[160-170]

It is usually important to know how much moisture is present in a filler and whether or not the filler is hygroscopic. Table 5.12 gives an overview of typical moisture concentration in some fillers (the fillers are qualified to a particular group based on their lower limiting value of the moisture concentration range). The information in the table is based on data for a large number of grades which vary in moisture content.

Table 5.12. Moisture in fillers

Moisture range, %	**Filler** (the range of moisture concentration for a filler is given in parentheses)
below 0.1	calcium carbonate (0.01-0.5), cristobalite (0.006-0.1), quartz (tripoli) (traces), wollastonite (0.02-0.6)
0.1-0.19	aluminum trihydroxide (0.1-0.7), barium sulfate (0.1-0.3), calcium sulfate (0.1), carbon black (0.12-2), glass fiber (0.1-3), graphite (0.1-0.5), iron oxide (0.1-3), fused silica (0.1), sand (0.1), talc (0.1-0.6)
0.2-0.39	antimony pentoxide (0.2-1), antimony trioxide (0.1), barium titanate (0.2), ceramic beads (0.2-0.5), diatomaceous earth (0.2-6), magnesium hydroxide (0.2-1), mica (0.3-0.7), titanium dioxide (0.2-1.5), zinc sulfide (0.3)
0.4-0.99	anthracite (0.5-4), perlite (0.5-1), fumed silica hydrophobic (0.5), fumed silica hydrophilic (0.5-2.5), sodium antimonate (0.5-3), zinc borate (0.4-0.5)
1-4.99	aluminum oxide (4-5), aramid fiber (1-8), attapulgite (2-16), bentonite (2-14), ball clay (3), calcium hydroxide (1.5), cellulose fiber (2-10), fly ash (2-20), kaolin (1-2), pumice (2), pyrophyllite (1), rubber particles (1), precipitated silica (3-7), slate flour (1), wood flour (2-12), zeolite (1.5)
5-9.99	hydrous calcium silicate (5.5-5.8), sepiolite (8-16)
above 10	calcium carbonate slurry (10-30), kaolin slurry (20-30), titanium dioxide slurry (10-20)

The presence of water in a filler is not usually beneficial. However, in paper manufacture and in water based paints, where aqueous slurries can be used, moisture level is of no major concern. Four benefits of using slurry are: lower cost, better dispersion, elimination of dust, and easier handling. The cost is reduced because the process of manufacture does not require drying which is an expensive step and packaging and handling is simpler with a slurry. Better dispersion contributes to improved quality in the final product due to the fact that slurries are usually stabilized to limit agglomeration. Whereas, when fillers are dried, the drying process results in the production of agglomerates. Environmental impact is reduced due to the fact that there is less waste and no packaging materials are involved. Drying processes burn large amounts of fuels and there are generally less environmentally friendly.

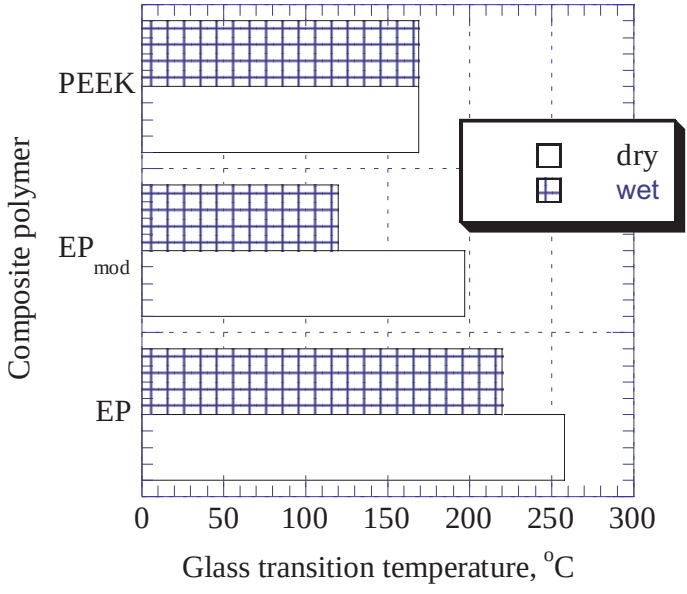

Figure 5.25. Glass transition of composites containing carbon fiber under dry and wet conditions. [Adapted, by permission from Selzer R, Friedrich K, *Composites, Part A*, **28A**, 1997, 595-604.]

In most other processes, the presence of moisture in filler either requires a process correction in the amount of the active ingredient or the moisture must be removed. In the case of hygroscopic fillers (which are very important to industry), the surface of the filler must be treated to lower moisture uptake. Montmorillonite,[167] glass beads and fibers,[165] silica,[164] titanium dioxide,[163] aramid fiber,[161] rubber particles,[169] and carbon fiber were studied to improve their moisture absorption and impart the hydrophobic properties.[160]

Figure 5.25 shows that the glass transition of composites containing carbon fibers may be affected by water uptake. The glass transition of carbon fiber/PEEK composite remains the same under dry and wet conditions. But carbon fiber/epoxy composites may experience a decrease in T_g as high as 77°C depending on the properties of the matrix resin.[160]

Composites containing aramid fibers rapidly regain moisture which results in a lowering their initial mechanical properties.[168] Figures 11.14 and 16.15 show the kinetics of moisture absorption by different fibers.[166] Figure 8.26 shows how moisture content affects compressive strength of aramid/epoxy laminates. Figure 5.26 shows the effect of moisture content on the interlaminar strength of epoxy/aramid laminates. Different fibers and epoxy resins were used in this study but the results follow a relationship of a linear decrease of adhesion as the moisture content decreases.

Figure 5.27 shows that a substantial amount of moisture is absorbed by glass beads/epoxy composites. The addition of glass beads increases the moisture uptake

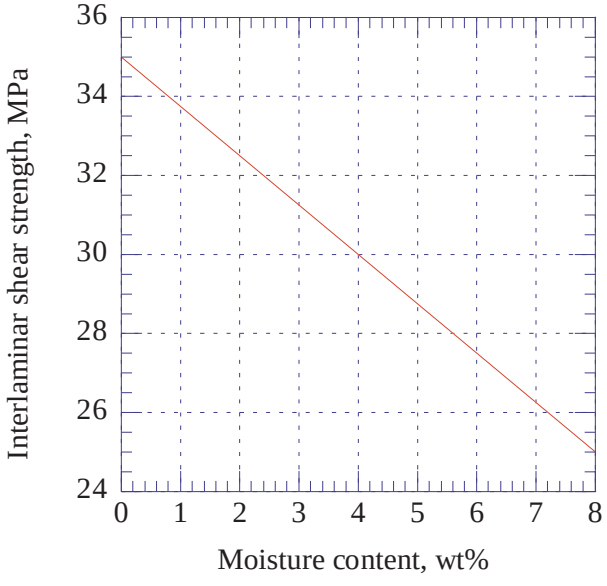

Figure 5.26. Interlaminar strength vs. moisture content in epoxy/aramid fiber laminates. [Data from Akay M, Mun S K A, Stanley A, *Composites Sci. Technol,* **57**, 1997, 565-71.]

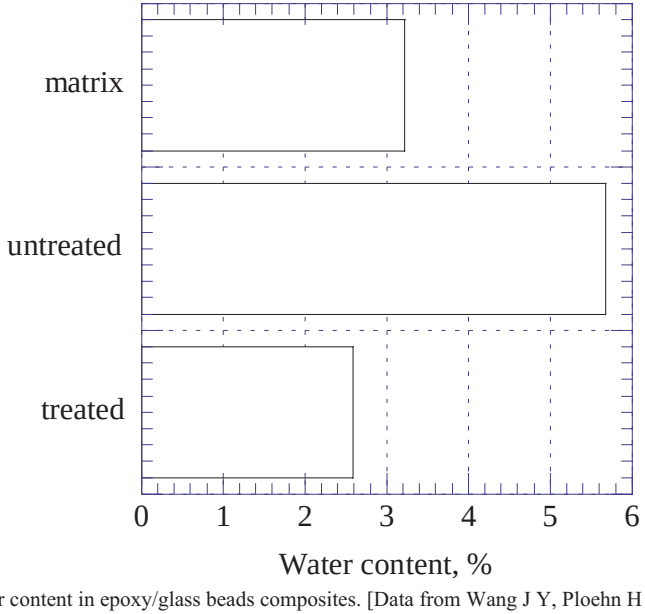

Figure 5.27. Water content in epoxy/glass beads composites. [Data from Wang J Y, Ploehn H J, *J. Appl. Polym. Sci.*, **59**, No.2, 1996, 345-57.]

over that of the plain matrix but a surface treatment of glass beads with silane decreases the water uptake to a value below the plain matrix.

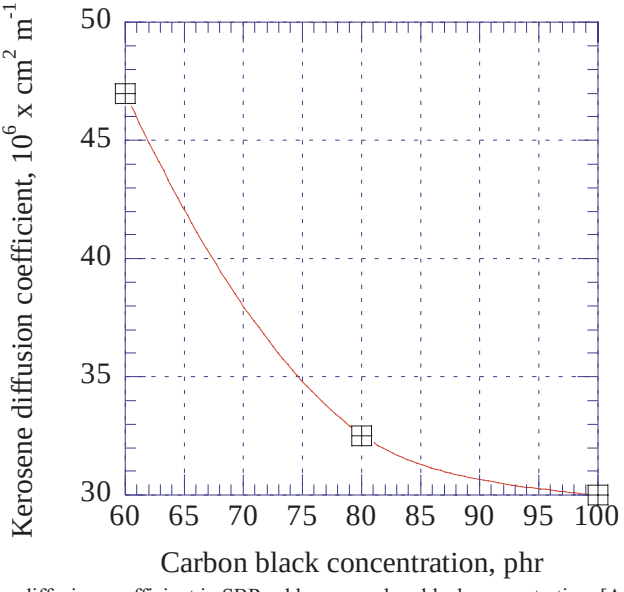

Figure 5.28. Kerosene diffusion coefficient in SBR rubber vs. carbon black concentration. [Adapted, by permission, from Nasr G M, Badawy M M, *Polym. Test.*, **15**, No.5, 1996, 477-84.]

In the rubber industry, moisture absorbed on the surface of silicate, impacts the rate and extent of cure and results in sponge-like textures. In moisture cured systems such as polyurethanes, polysulfides and silicones, moisture causes a premature reduction in shelf-life. In extrusion and injection molding the moisture absorbed on fillers contributes to various defects and a strict regime must be followed regarding the drying time and the conditions prior to processing. Lacing, a less well known phenomenon, is caused by the absorption of moisture on the surface of titanium dioxide.[163]

5.18 ABSORPTION OF LIQUIDS AND SWELLING[171-189]

Information on absorption of liquids and gases by filled materials remains limited even though it is very important to two areas of applications: filled reactive systems and solvent resistant materials.

In the study of precipitated silica grades (Zeosil), the absorption of four different amines was studied. The effect of the amine type on absorption was generally stronger than the silica grade but the absorption of all grades of silica increased when the concentration of functional groups (OH) on the surface was increased. Two grades had higher absorption levels because they had a pH below seven. Extraction by water removed a large part of the absorbed amine but 10-20% of the initial amine concentration always remained absorbed. This study may explain some reasons for retarded and incomplete cures in systems which contain fillers.

A mathematical model was proposed for evaluating the diffusion of a material which can react with the filler (e.g., acid). The proposed method permits the study of process kinetics for different concentrations of penetrant and filler.[179]

SBR filled with intercalated montmorillonite had substantially lower toluene uptake compared with the same rubber filled with carbon black (see Figure 15.42). Figure 5.28 shows that the diffusion coefficient of kerosene, which defines penetration rate, decreases when the concentration of carbon black in SBR vulcanizates is increased.[176] Figure 15.33 compares the uptake rate of benzene by unfilled rubber and by silica and carbon black filled rubber. Both fillers reduce the solvent uptake but carbon black is more effective.

Similarly, swelling of polyethylene filled with 35 and 50 wt% calcite was reduced. Table 5.13 gives equilibrium swelling of polyethylene in different solvents.

Table 5.13. Equilibrium swelling of calcite-filled polyethylene. Data from Ref.[178]

Solvent	HDPE	HDPE+35 wt% calcite	HDPE+50 wt% calcite
heptane	4.0	3.8	2.7
o-xylene	6.7	5.3	4.7
tetrachloroethylene	14.0	10.8	6.7

The swelling rate of polybutadiene/carbon black mixtures was reduced when the mixture was swollen, dried and swollen again.[182] This experiment, together with other studies conducted by NMR, explains the reasons for the reduction in swelling polymer/filler composites. As discussed in Chapter 7, the addition of filler and its interaction with polymer results in a bound fraction of polymer on the filler surface. During mixing, the interaction between the polymer and the filler surface is a chaotic process which causes the surface of filler to be incompletely covered by interacted chain segments. Swelling increases chain mobility and allows the chains to rearrange themselves to provide a more perfect coverage which increases the amount of bound polymer. The bound polymer fraction is then more difficult to swell which reduces the rate of solvent diffusion.

An increase in concentration of carbon fiber in SBR reduced the swelling rate but increased swelling anisotropy. Longer fibers (6 and 1 mm long fibers were studied) were more effective in the reduction of swelling in length direction but have almost no influence on swelling in the width direction. Increased anisotropy of swelling with fiber loading is explained by the increased fiber orientation with loading which thus only affects swelling behavior in the direction of orientation.

5.19 PERMEABILITY AND BARRIER PROPERTIES[190-197]

Plate like particles act as a barrier to gas diffusion by increasing the tortuosity of the diffusion pathway according to the following equation:

$$\frac{P_c}{P_p} = \frac{\phi_f}{1 + (W / 2T)\phi_p} \qquad [5.24]$$

where

P_c	permeability of composite
P_p	permeability of unfilled polymer
ϕ_p	volume fraction of polymer
ϕ_f	volume fraction of filler
W	particle width
T	particle thickness

Figure 15.22 shows the effect of changes in the volume fraction of clay on CO_2 permeability. Permeability decreases most dramatically when the aspect ratio (particle width divided by particle thickness, W/T) is increased.[191] Figure 19.20 gives an example of the effect of talc loading on the oxygen permeability of HDPE film.[195,197] The practical application of mica in corrosion resistant coatings is widespread. The same principles apply to both liquids and gases. Section 5.12 gives the ranges of aspect ratios of available fillers.

Limiting the diffusion of oxygen improves the weather stability of materials due to reduced photooxidation.[194] This subject is discussed in Chapter 11.

There is still another aspect of permeability which has an influence on the durability of coatings. This is partially related to critical pigment volume concentration, CPVC (see Section 5.13 in this chapter) but it is also related to pigment-filler interaction relative to surface energy. A study on the effect of titanium dioxide on durability of coatings, containing different grades of titanium dioxide with different PVCs, shows that an increase in PVC decreases the resistance of the coating to salt spray but durability was also related to the grade of titanium dioxide used.[190] If the titanium dioxide did not have any surface coating, specimens of coatings cracked at very low concentration of pigment (PVC=6.4) well below the CPVC. By comparison, coatings containing titanium dioxide coated with Al_2O_3 and SiO_2 did not crack at PVC=17 which is slightly above the CPVC. This shows that permeability is also governed by pigment-filler interactions and the effect that a pigment has on the durability of a binder.

Fillers influence the performance of semi-permeable membranes. Semi-permeable membranes were obtained by stretching a highly filled film.[192] In another application, zeolites were used to obtain polymer membranes used in gas separation.[193]

5.20 OIL ABSORPTION

Oil absorption is a widely used parameter to characterize the effect of filler on rheological properties of filled materials. If oil absorption is low, the filler has little effect on the viscosity. The effect of particle shape on rheology should be considered

since it is known that spherical particles aid flow due to their ball bearing effects. Fillers which have medium oil absorption are useful as co-thickeners. Filler having a very high oil absorption are used as thickeners and absorbents. Particle morphology (see Chapter 2 to view different morphological structures) may contribute to high oil absorptions (several hundred times the mass of filler) if the particles have exceptionally high porosities. Oil absorption must also be considered in applications which need filler for reinforcement.

The reinforcement by fillers increases as the filler concentration increases since the reinforcing mechanism is related to the presence of active sites on the filler surface which are available for reaction or interaction with matrix polymer. But this increase is limited by the effect a filler has on the rheological properties of a mixed material. There is a certain filler concentration above which the reinforcing effect of the dispersed filler is lost. Carbon black can serve as a simple example. Acetylene black has many useful properties but it cannot be used effectively for reinforcement because its structure does not permit high loadings whereas some furnace blacks can be loaded to high concentrations.

Table 5.14 gives an overview of oil absorptions. The oil absorptions are based on various grades to show the available variety.

Table 5.14. Oil absorption of fillers

Oil absorption range, g/100 g	**Filler** (the range for a particular filler group is given in parentheses)
below 10	barium sulfate (8-28), barium & strontium sulfates (9.5-11.5)
10-19.9	aluminum trihydroxide (12-41), calcium carbonate (13-21), ferrites (10.8-14.8), glass beads (17-20), iron oxide (10-35), fused silica (17-27), quartz, tripoli (17-20), sand (14-28), titanium dioxide (10-45), wollastonite (19-47), zinc sulfide (13-14)
20-29.9	aluminum oxide (25-225), cristobalite (21-28), feldspar (22-30), kaolin (27-48), slate flour (22-32), talc (22-57)
30-49.9	barium metaborate (30), ball clay (36-40), bentonite (36-52), carbon black (44-300), magnesium hydroxide (40-50)
50-100	attapulgite (60-120), graphite (75-175), kaolin beneficiated (50-60) kaolin calcinated (50-120), mica (65-72), precipitated silica (60-320), silica gel (80-280), wood flour (55-60)
over 100	cellulose fiber (300-1000), diatomaceous earth (105-190), fumed silica (100-330), hydrous calcium silicate (290), perlite (210-240)

5.21 HYDROPHILIC/HYDROPHOBIC PROPERTIES[147,198-199]

In water-based systems, it is important that the filler is compatible with water, usually, filler dispersion occurs in an aqueous medium before a polymer emulsion is added. The manufacturers of fillers for water-based systems frequently provide a simple demonstration of the change in the filler's hydrophobicity by comparing the

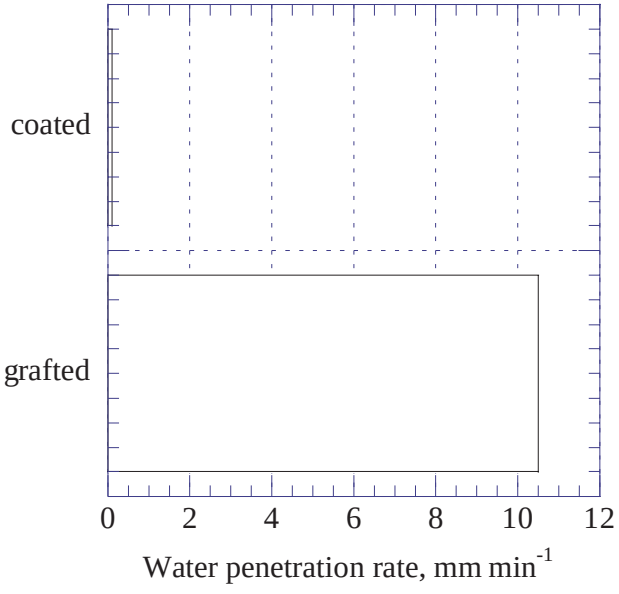

Figure 5.29. Penetration rate of water through column packed with grafted and stearate coated barium sulfate. [Adapted, by permission, from Tsubokawa N, Seno K, *J. Macromol. Sci. A*, **31**, No.9, 1994, 1135-45.]

unmodified filler which floats on water with the modified filler which mixes readily with water. There are numerous methods of increasing hydrophilic properties of fillers. These include grafting, surface coating, oxidation, etc. Figure 5.29 demonstrates the results of acrylamide grafted on the barium sulfate in comparison with stearate coated barium sulfate. These two products display a spectacular difference in behavior since the stearate coated barium sulfate floats on water in spite of the fact that its density is four times higher than that of water while the acrylamide grafted product readily sinks into water and mixes without difficulties. The penetration rate of water through a column packed with filler provides a method of quantifying these observations. Surface grafting with a hydrophilic polymer gives a substantial improvement in the compatibility of the filler and water.[147]

However, the hydrophilic surface of fillers is often a serious disadvantages, considering that the majority of polymers are hydrophobic. This single feature frequently diminishes the economic advantage gained from the use of relatively inexpensive filler because the cost of its dispersion outbalances the reduced cost of the material. Two research groups in Poland[198,199] contributed data which shows the broad spectrum of possibilities of filler modifications. The results of filler modification were quantified by using the degree of hydrophobicity calculated from the following equation:

$$N = 100(mH_i^B - nH_i^B) / mH_i^B \qquad [5.25]$$

where
mH_i^B heat of immersion in benzene of modified filler
nH_i^B heat of immersion in benzene of unmodified filler

The heats of immersions were measured in a differential calorimeter. Table 5.15 gives data for 2 wt% coating of the filler surface. More detailed information can be found in the original papers which, in addition to the full calorimetric data for 1, 2, and 3 wt% coatings, gives a set of mechanical properties of rubber vulcanizates and polyurethanes containing these modified fillers. Also, results for proprietary coatings are given which demonstrate the further improvement of quality in such fillers.

Table 5.15. Degree of hydrophobicity of various fillers. Data from refs. 198 and 199

Surface modifier	Chalk	Precipitated $CaCO_3$	Kaolin	Precipitated SiO_2
stearic acid	20.1	21.7	9.2	
magnesium stearate	21.1	20.1		
calcium stearate	20.7	20.1	8.3	
oleic acid	21.1	23.0		
tall oil	22.7	21.7		
tetrabutylammonium chloride	23.7	22.6	26.2	
sodium dodecylsulfate	11.9	21.7	14.4	
sodium glutamate	13.8	23.6		
polyethylene glycol (10,000)	9.8	8.4	15.4	
mecaptosilane (A-189)	8.2	4.6	27.8	24.6
aminosilane (A-1100)	5.6	3.4	18.5	
isostearoil titanate (KRTTS)	26.6	29.1	31.8	
9-butyl-3,6-dioxa-azatridecanol				27.3
3.6-dioxa-9-thiaheptadecanol				25.9
7,10,13,16-tetrathiadocosane				23.8

The fatty acid derivatives give a very good performance on calcium carbonate but are inferior on kaolin. The results of mechanical testing show that the ease of dispersion and mechanical properties of fillers are governed by interactions with the matrix polymer. Thus, mechanical testing of the filled material must be carried out before the best coating can be selected for a given polymer.

5.22 OPTICAL PROPERTIES[200-208]

Gloss and brightness are the most important indicators of paints and paper quality. Fillers and pigments influence both properties. The gloss of paper depends on the amount of pigment (relative to the coat weight) and the amount of thickener. The surface gloss of paints depends primarily on the film-forming properties of the resin although fillers may also influence gloss if they cause surface roughening (see Sections 5.4 and 5.13). Since gloss is the result of surface smoothness, the degree of pigment dispersion has an impact.[200] The paint formulation should be designed to assist dispersion of fillers and pigments but it should also include consideration of the processes occurring during drying. Two stages of paint drying are distinguished.[201] The first, wetter, stage involves removal of the majority of solvent. Surface tension dominates this stage. The surface of the drying film remains smooth. Surface tension remains constant throughout the drying process, and the compressive strength of the structure during the first stage is lower than the surface tension. In the second stage, the compressive strength and the yield stress increase until they exceed the surface tension. The yield stress of high gloss paint increases slower than that of low gloss paint. If the film shrinks, surface roughness develops.

As TiO_2 concentration increases, gloss increases because increasing the concentration of this pigment increases the refractive index. But, conversely gloss decreases as the amount of pigment increases because particulates roughen the surface. So the two mechanisms compete. In flocculated systems, the structure develops earlier during the drying process than in paints containing well-dispersed pigments. An increase in gloss and color strength follows the dispersion of coarse agglomerates.[202] During the service life of a paint, the gloss changes because of chalking – a phenomenon related to binder degradation. A degraded surface contains a particulate deposit which affects light reflection.[204] In black ink formulations, gloss mostly depends on particle size and the structure of carbon black. Smaller particle diameter and low structure of carbon black help to give the high gloss to black inks.

Brightness can be affected by fillers. The tables for individual fillers in Chapter 2 contain information on brightness. In white coatings, a yellowish undertone may be caused by binder or by fillers. This undertone can be eliminated by the addition of small quantities of a blue or violet pigment, carbon black with bluish tinge or fine particles of aluminum powder.[134] But such correction usually causes a loss of brightness. If optical brighteners are used, a loss of brightness can be avoided.

The hiding power of the pigmented material is a measure of its ability to hide a colored substrate or differences in the substrate color. The hiding power of the film is determined from the following equation:[134]

$$CR = L^*_B \,/\, L^*_w \qquad [5.26]$$

where
CR contrast ratio

L^*_B brightness over a black substrate
L^*_w brightness of a white substrate

According to DIN 53 778, the coating is considered fully opacifying if the contrast ratio, CR≥0.98. In inks and paints, hiding power or tinting strength is the most important factor characterizing the quality of the pigment. Particle size distribution is the major factor affecting the tinting strength of a filler. The type of filler, in conjunction with other components of the composition, determines the processes occurring during storage. Flocculation of pigment is usually responsible for a change of the initial hiding power.

In printing inks, which are pigmented with carbon black, the tone can be corrected by the choice of carbon black type. Since the tinting strength increases when the particle size and structure of carbon black decrease, the natural tendency is to use material of a very fine particle size. Black inks are usually required to have a blue tone, which is contrary to the choice of carbon black based on the particle size, because as the particle size decreases, the brown tone becomes more pronounced.

5.23 REFRACTIVE INDEX

Refractive index influences light scattering in fillers and pigments. A correct choice in the refractive index of the particulate material and binder permits a formulation of transparent materials containing fillers (for further information on light scattering see Chapter 2, especially section on titanium dioxide and Section 5.3). Table 5.16 gives an overview of refractive indices of various fillers.

Table 5.16 Refractive indices of fillers

Refractive index range	**Filler** (refractive index of a particular group of fillers is given in parentheses)
1	air (1)
1.3-1.49	calcium carbonate - calcite (birefringence: 1.48 & 1.65), cristobalite (1.48), diatomaceous earth (1.42-1.48), fumed silica (1.46), precipitated silica (1.46)
1.5-1.69	aluminum trihydroxide (1.57-1.59), attapulgite (1.57), barium metaborate (1.55-1.6), barium sulfate (1.64), calcium hydroxide (1.57), calcium sulfate (1.52-1.61), feldspar (1.53), glass beads, flakes and fibers (1.51 A-glass and 1.55 E-glass), hydrous calcium silicate (1.55), kaolin (1.56-1.62), magnesium hydroxide (1.56-1.58), mica (1.55-1.69), perlite (1.5), pyrophyllite (1.57), quartz (1.56), talc (1.57-1.59), wollastonite (1.63), zinc borate (1.59)
1.7-1.99	aluminum oxide (1.7), antimony pentoxide (1.7), calcium carbonate - aragonite (1.7), magnesium oxide (1.736), sodium antimonate (1.75), zinc stannate (1.9)
2-2.19	antimony trioxide (2.087), zinc oxide (2)
2.2 and above	barium titanate (2.4), iron oxide (2.94-3.22), titanium dioxide (2.55-2.7), zinc sulfide (2.37)

The fillers in the Table 5.16 are divided into six groups. The first group includes air which is a good "pigment" because the difference in refractive index between air and most binders is in the range of 0.4-0.6 therefore it has a scattering power comparable to zinc oxide. The second group consists of fillers which are the most suitable materials for transparent products since their refractive indices fall into a range similar to many polymers. The third group consists of typical fillers. Even if they have a white color, their contribution to coloring is very small because of the small difference between their refractive index and that of binder. It is considered that material is a pigment if its refractive index is above 1.7 which is the case of the last three groups. The last group contains the most important white pigments. Because of its very high refractive index, titanium dioxide has the highest scattering power of white pigments.

5.24 FRICTION PROPERTIES[209-214]

Fillers are available with a range of frictional properties from self-lubricating through severely abrasive which permits applications which range from slide bearings to brake pads.

Polytetrafluoroethylene, molybdenum disulfide, graphite, and aramid fibers reduce the frictional coefficient. These may be used as single friction additive, in combination with other fillers, and in combination with silicone oil. Table 5.17 illustrates effect of PTFE on the frictional properties of different polymers.

Table 5.17. Wear factor and dynamic coefficient of friction of different polymers containing PTFE Polymist. *Courtesy of Ausimont USA, Inc.*

Polymer	PTFE, %	Wear factor		Dynamic coefficient of friction	
		Unmodified	Modified	Unmodified	Modified
POM	20	65	15	0.21	0.15
ECTFE	10	1000	27	0.29	0.11
PA-6	20	200	15	0.26	0.19
PA-66	20	200	12	0.28	0.18
PC	20	2500	70	0.38	0.14
PBT	20	210	15	0.25	0.17
PPS	20	540	55	0.24	0.10
PU	15	340	60	0.37	0.32

The coefficient of friction and wear are substantially reduced by the incorporation of PTFE powder. Molybdenum disulfide has an even broader range of application temperatures than PTFE (-150 to 300^{o}C, PTFE up to 260^{o}C) and provides even better performance under high load. For this reason it is used either in combination

with PTFE or alone. Aramid fibers give additionally reinforcement therefore are frequently found in combinations with other fillers.

Many fillers play a prominent role in brake pads and clutch linings. These include fibers such as aramid, glass, carbon, steel, and cellulose; low cost fillers such as barites, calcium carbonate and clay; frictional modifiers such as alumina, metallic flakes and powders. The combination of these materials with binders gives a broad range of brake pad materials.

Numerous other materials are used as a components of proprietary polishing and abrasive materials with a variety of uses.

5.25 HARDNESS[8,215,216]

Hardness of fillers is summarized in Table 5.18.

Table 5.18. Hardness of fillers

Mohs hardness	**Filler** (the range for a particular filler is given in parentheses)
1	attapulgite (1-2), bentonite (1-2), carbon fibers (0.5-1), graphite (1-2), molybdenum disulfide (1), precipitated silica (1), pyrophyllite (1-2.5), talc (1-1.5)
2	aluminum flakes and powder (2-2.9), aluminum trihydroxide (2.5-3.5), anthracite (2.2), calcium sulfate (2), clay (2-2.5), copper (2.5-3), gold (2.5-3), kaolin (2), mica (2.5-4), sepiolite (2-2.5), silver (2.5-4)
3	barium sulfate (3-3.5), calcium carbonate (3-4), dolomite (3.5-4), iron oxide (3.8-5.1), lithopone (3), zinc sulfide (3)
4	calcinated kaolin (4-8), wollastonite (4.5), zinc oxide (4)
5	apatite (5), ceramic beads (5-7) perlite (5.5), pumice (5.5), silver-coated, light glass spheres (5-6), titanium dioxide - anatase (5-6)
6	cristobalite (6.5), feldspar (6-6.5), glass beads, flakes and fibers (6 for A-glass and 6.5 for E-glass), silica gel (6), titanium dioxide - rutile (6-7)
7	fused silica (7), silver-coated, thick-wall glass spheres (7), quartz (7), sand (7)
9	aluminum oxide (9), carborundum (9-10), tungsten powder (9)

The most popular fillers are soft materials in the hardness range of 1-3. Silica fillers are hard and frequently abrasive. Most grades of silicas have a hardness in the range 6-7.

The effect which fillers have on the hardness of filled materials is detailed in the data in Figure 5.30. Graphite is a soft material but still it may either increase or decrease the hardness of a polymer depending on its interaction and particle size. In polyamide-66, small particle size graphite increases hardness while coarse particles have little influence on the hardness of the composite. In polypropylene, all grades of graphite substantially increase hardness. But with polystyrene (not shown here), hardness is decreased by all grades of graphite. The effect depends on the interaction between polymer and filler.

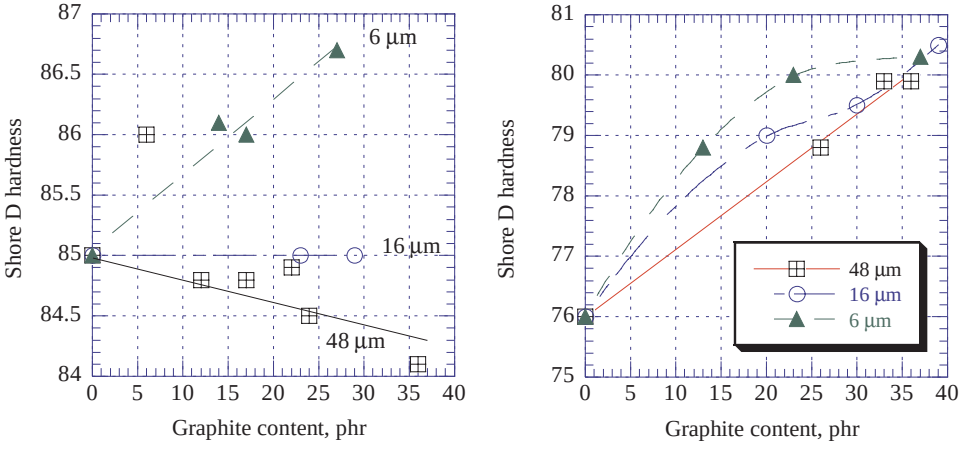

Figure 5.30. Hardness of composite vs. graphite concentration and type. Left -PA-66, right - PP. *Courtesy of Timcal Ltd., Sins, Switzerland*.

The general trend in filled material is that fillers increase hardness as the filler concentration is increased. In highly filled materials, especially those filled with silica flour, the hardness of the composite approaches the hardness of the filler. Several different fillers were found to induce a softening effect in aged PDMS.[215] While a freshly prepared composite increased in hardness as the filler concentration was increased, the aged material reached a minimum hardness around 20 wt% filler. The hardness then increased gradually as the spaces between particles were taken up by the filler.[215]

5.26 INTUMESCENT PROPERTIES[217-220]

Natural graphite brings intumescence to products used in construction and other applications where fire retardancy is important. The growing interest in intumescent products stems from findings that the most effective method of decreasing the combustibility of plastics is to use additives which cause carbonization of the organic materials. The material should also retain the formed gases and expand to built an insulating layer.

A combination of materials must be used to regulate the kinetics of such processes as degradation, gas formation, char formation, and foam growth. The major components include a carbonization catalyst, a carbonization agent, and a blowing agent. These components are designed to form gaseous products which cause expansion of the product (e.g., coating or sealant). The design of the product must also include mechanisms which allow it to retain these formed gases. With foams the pressure in the bubble must be balanced by the surface tension and mechanical properties of the bubble wall for the gas to be retained. For this reasons, it is important to design composition which changes its properties under increasing heat to re-

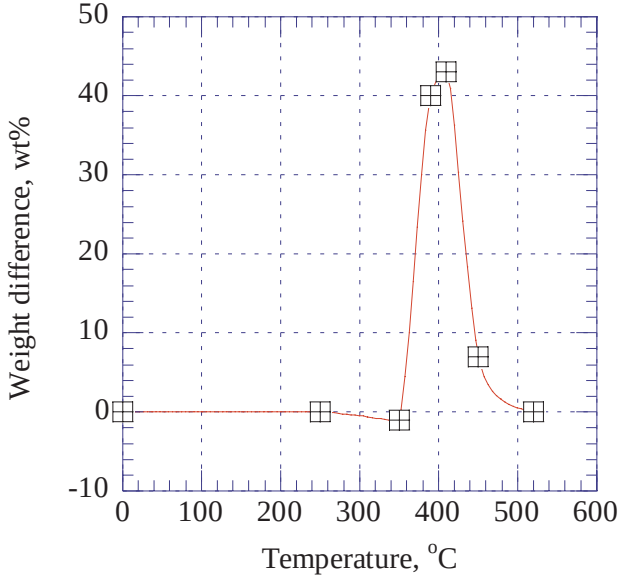

Figure 5.31. Weight difference of intumescent formulation based on LDPE vs. temperature. [Adapted, by permission, from Le Bras M, Bourbigot, Le Tallec Y, Laureyns J., *Polym. Degradat. Stabil*., **56**, 1997, 11-21.]

tain sufficient mechanical properties such that gas is retained. Both the resin and the filler play a part in this process.

The success of graphite in this applications shows that filler with plate like structures should be considered when intumescent materials are being formulated. Recent developments in intumescent paints[219] show that performance can be improved if a layer of organic material is inserted between the layers of the plate like filler. The degradation of this material in the enclosed space increases the expansion rate and the retention of gas inside the degrading material. Based on this principle any plate like filler has the potential to be useful in an intumescent application. The composition of filler is also important. When clay was used as a filler in fire retardant applications, it was found that some of its components interfere with the action of carbonization catalysts and detract from the overall performance of the system in terms of limiting oxygen index.[218]

Figure 5.31 shows a curve typical of the performance of intumescent material. The degradation process should occur rapidly which generates an insulation layer in a short period of time and keeps the temperature of adjacent layers sufficiently low to prevent their degradation. In the graph, the height of peak is important since it shows the amount of retained material.

5.27 THERMAL CONDUCTIVITY[78,126,189,221-230]

Table 5.19 gives an overview of the thermal conductivity of various fillers. The data in the table is skewed towards thermal insulators at one and at thermal conduc-

tors at the other range since data for other fillers are seldom available because they are not intended for heat insulating or conducting applications. In most cases, non-metallic fillers are thermal insulators but pitch-based carbon fiber is the exception. It has a higher thermal conductivity than any metal.

Table 5.19. Thermal conductivity of fillers

Thermal conductivity range, W/K·m	**Filler** (thermal conductivity given in parentheses)
below 10	aramid fiber (0.04-0.05), calcium carbonate (2.4-3), ceramic beads (0.23), glass fiber (1), magnesium oxide (8-32), fumed silica (0.015), fused silica (1.1), molybdenum disulfide (0.13-0.19), PAN-based carbon fiber (9-100), sand (7.2-13.6), talc (0.02), titanium dioxide (0.065), tungsten (2.35), vermiculite (0.062-0.065)
10-29	aluminum oxide (20.5-29.3), pitch-based carbon fiber (25-1000)
100-199	graphite (110-190), nickel (158)
above 200	aluminum flakes and powder (204), beryllium oxide (250), boron nitride (250-300), copper (483), gold (345), silver (450)

Figure 15.17 shows that high aspect ratio carbon fibers are used to make materials electrically conductive. Figure 15.19 shows that thermal conductivity depends only on the amount of carbon fibers, not on their length or aspect ratio.[126] Mathematical modelling which shows that high aspect ratio fibers should increase thermal conductivity but some practical experiments disprove this.[221] Several other models analyzed in a review paper[224] are in agreement with the experimental data and this analysis confirms that the thermal conductivity of filler and its concentration are the main parameters determining the thermal conductivity of composite.[224] A composite based on epoxy resin (60 parts) and pitch-based carbon fiber (40 parts) had a thermal conductivity of 540 W/K·m which is higher than the thermal conductivity of metal. In another study,[225] the thermal conductivity of HDPE filled with aluminum particles was found to be 3.5 W/K·m.

In modern electronic devices there is a need to manufacture materials which have high thermal conductivity and a high electrical resistance. The data in the Table 5.19 show that such a requirement can be easily fulfilled using boron nitride or beryllium oxide. Both fillers have excellent thermal conductivity and they are electrical insulators.

Some of the insulating fillers found in the first row of Table 5.19 are used in foams and adhesives designed for insulation in modern appliances.[229,230]

5.28 THERMAL EXPANSION COEFFICIENT[231-234]

Table 5.20 contains data on the linear thermal expansion coefficient of various fillers. The data indicate that most fillers, especially these used for reinforcement, have much lower coefficient of thermal expansion than metals and plastics. This is an important fact which should be considered in formulating plastics exposed to

wide temperature swings since one of the requirements of filler addition is to reduce thermal expansion and improve dimensional stability of plastics. This data also shows that it is preferable to use mineral fillers for thermally conductive plastics because they have low thermal expansion coefficient.

Table 5.20. The linear thermal expansion coefficient, α, of different fillers in temperature range of 20-200°C

α range, 10^{-6} K^{-1}	**Fillers** (the value of α for a particular group of fillers given in parentheses)
below 5	aramid fiber (-3.5), boron oxide (<1), calcium carbonate (4.3-10), calcinated kaolin (4.9), carbon fiber (-0.1 to -1.45), fused silica (0.5), glass beads and fiber from E-glass (2.8), pyrophyllite (3.5)
5-9.9	beryllium oxide (9), glass beads and fiber from A-glass (8.5), mica (7.1-14.5), talc (8), titanium dioxide (8-9.1), wollastonite (6.5)
10-14.9	barium sulfate (10-17.8), dolomite (10.3), magnesium oxide (13), molybdenum disulfide (10.7), quartz (14), sand (14)
15-19.9	feldspar (19)
20-29.9	aluminum flakes and powder (25)
30-100	cristobalite (56)

Thermal expansion can be used as simple method of verifying the adhesion between the filler and the matrix. If the adhesion is poor the composite will have high thermal expansion.[232]

5.29 MELTING TEMPERATURE

Melting temperatures of fillers are given in the tables for individual fillers in Chapter 2. These temperatures are usually so high that they do not have much relevance to filler choice. The only area when the melting or decomposition temperature of the filler may become relevant is in the processes of filler recovery from waste plastics. Such studies were not found in the literature.

Fillers such as magnesium hydroxide and aluminum trihydroxide are used as flame retardants because their decomposition product – water – is an active ingredient in flame retardancy. These fillers are discussed in detail in Chapter 12.

5.30 ELECTRICAL PROPERTIES[4,8,52,75,78,89,102,126-7,177,185-6,189,204,224,234-272]

One single property of filler – electric conductivity – affects many properties of the final products. These properties include electric insulation, conductivity, superconductivity, EMI shielding, ESD protection, dirt pickup, static decay, antistatic properties, electrocatalysis, ionic conductivity, photoconductivity, electromechanical properties, thermo-electric conductivity, electric heating, paintability, biocompatibility, etc. Possession of one of these properties in a polymer can make it useful in industry and everyday use. Examples are given in Chapter 19. Here, the electrical

properties of fillers are summarized and the general effect of a filler's conductivity on the properties of filled materials is analyzed.

Table 5.21. Electrical properties of fillers

Filler	Resistivity Ω-cm	Dielectric constant	Dielectric strength V/cm	Loss tangent
Aluminum	2.8×10^{-6}			
Aluminum oxide	10^{14}-10^{22}	9-9.5	2560	0.0002-0.004
Aluminum trihydroxide		7		
Anthracite	50			
Barium sulfate	19.075	11.4		
Barium titanate		3.8		
Beryllium oxide	10^{17}	6.8	100	0.0004
Boron nitride	10^{15}	3.9		<0.0002
Calcium carbonate	10^{10}	6.1-8.5		
Carbon fiber	10^{-2}-10^{-5}			
Carbon fiber, Ni-coated	6×10^{-6}			
Ceramic beads		1.6		
Copper	1.6×10^{-6}			
Ferrites	10^{2}-10^{10}	8-22		
Fumed silica	10^{13}			
Fused silica	10^{17}-10^{18}	3.78		0.001
Glass beads	10^{7}	1.2-7.6	4500	0.015-0.058
Glass fibers	10^{13}-10^{16}	5.8-6.1		0.001
Gold	2.1×10^{-6}			
Graphite	0.8-2.5			
Kaolin		1.3-2.6		
Mica				0.0013-0.04
Nickel	7.8×10^{-6}			
Precipitated silica	10^{11}-10^{14}	1.9-2.8		0.00001-0.02
Sand	10^{14}-10^{16}	4		0.0002
Silver	1.6×10^{-6}			
Steel	72×10^{-6}			
Talc		7.5		
Titanium dioxide	$3\text{-}9 \times 10^{3}$	48 (anatase) 114 (rutile)		0.01-0.35
Tungsten	5.6×10^{-6}			

Table 5.22 gives resistivity and dielectric constants of selected polymers.

Table 5.22. Resistivity and dielectric constants of some polymers

Polymer	Resistivity, Ω-cm	Dielectric constant
Epoxy resin	10^{12}-10^{14}	3.5-6
Polyethylene	>10^{15}	2.3
Polypropylene	>10^{15}	2.2-2.6
Polystyrene	>10^{16}	2.5-2.65
Polytetrafluoroethylene	10^{18}	2
Polyvinyl chloride	10^{12}-10^{16}	3.2-4
Silicone	>10^{12}	3.5

When the two tables are compared it is evident that there is a wide choice in fillers which either enhance or retain dielectric properties of polymers. It is more difficult to formulate conductive polymers where consideration must be given to how the filler can change properties of the polymer. Electrically conductive polymers can be divided into three groups:[255]

	resistivity range, Ω-cm	**applications**
low conductors	10^{6}-10^{11}	antistatic protection
semi-conductors	10^{2}-10^{6}	EMI shielding, ESD dissipation
conductors	below 10^{2}	heaters, sensors, elastic conductors

Comparing the range of conductivity of low conductors with resistivity of some fillers in Table 5.21 shows that the task of their formulation is not difficult.

For EMI shielding applications, numerous processes are used, some require conductive fillers. These applications include parts molded with conductive filler and conductive paints. Conductive fillers used in commercial applications include aluminum, silver, nickel, and copper flakes and powders, stainless steel fibers, and fibers and flakes coated by nickel and silver. Thermoplastic compounds can provide up to 65-70 dB of electromagnetic noise attenuation but obtaining values over 45 dB is difficult. Static dissipative compounds (ESD) are mostly produced with carbon black which accounts for approximately 90% of the market but many other fillers are also used.

Several general principles determine the amount of filler which must be incorporated. Figure 5.32 shows a typical relationship between the concentration and conductivity. The initial addition of conductive fillers does very little to the change of conductivity until a threshold concentration or percolation threshold is attained.

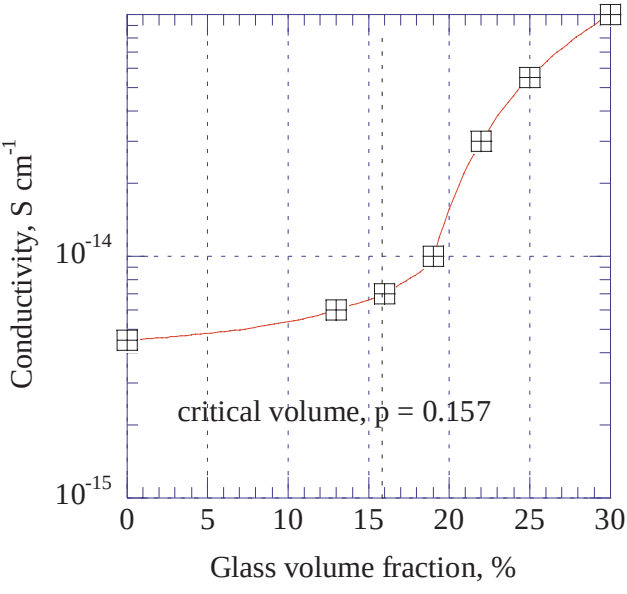

Figure 5.32. Conductivity of epoxy resin filled with silver coated glass beads vs. volume concentration. [Adapted, by permission, from Lekatou A, Faidi S E, Lyon S B, Newman R C, *J. Mat. Res*., **11**, No.5, 1996, 1293-304.]

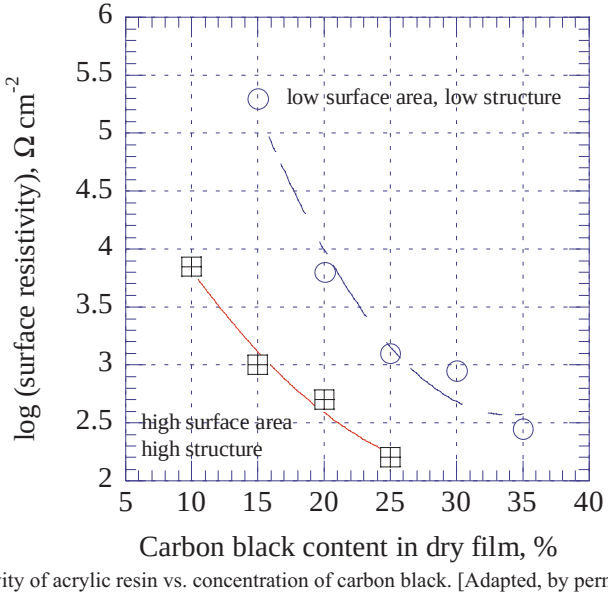

Figure 5.33. Resistivity of acrylic resin vs. concentration of carbon black. [Adapted, by permission, from Foster J K, Sims E S, Venable S W, *Paint & Ink Int*., **8**, No.3, 1995, 18-21.]

The amount of filler required to reach this threshold value depends on the conductivity of the particular filler, its particle shape, and its interaction with matrix. After percolation threshold, conductivity increases rapidly. The steepness of the increase

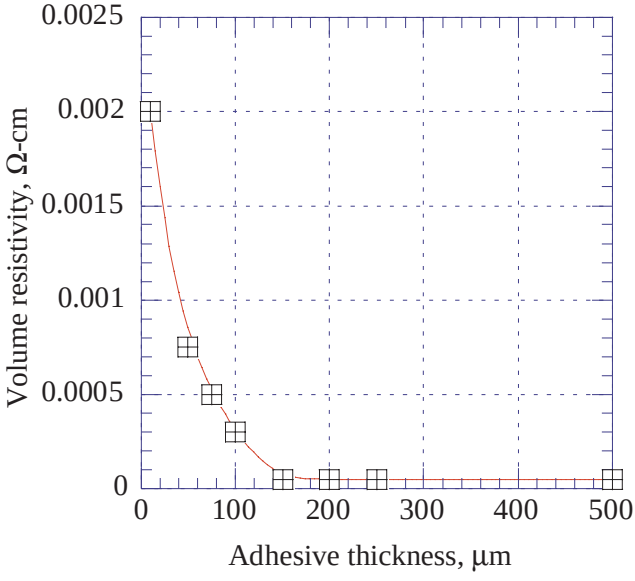

Figure 5.34. Resistivity vs. adhesive layer thickness. [Adapted, by permission, from Wei Y, Sancaktar E, *J. Adhesion Sci. Technol*., **10**, No.11, 1996, 1199-219.]

is controlled mostly by the particle shape and the intrinsic conductivity of the filler. Finally, the conductivity reaches a plateau the value of which depends both on the conductivities of the filler and the matrix.

Particle size, and in the case of carbon black, its structure, and the amount used determine the properties of the filled composite (Figure 5.33). The smaller the particle and the higher the structure, the less carbon black is required. The same holds true for particulate materials (see Figures 15.10 and 15.37).

A third important filler parameter is related to its shape. Figure 15.17 shows that the aspect ratio of carbon fiber affects conductivity. If the fiber is milled to almost spherical particles, its percolation threshold concentration is substantially increased.

In very thin conductive layers such as adhesives, paints or inks, the layer thickness plays a big part (Figure 5.34).[267] The graph shows that a certain thickness is required before a full conductivity effect is obtained.

5.31 MAGNETIC PROPERTIES[273-279]

Two other sections are devoted to the magnetic properties of fillers. Filler materials are discussed in Section 2.1.29 and some examples of such products are included in Section 19.23. Figure 5.35 shows that fiber orientation strongly influences magnetic properties. Figure 5.36 shows that the shape of the manufactured article may determine how the filler particles are oriented. This, in turn may determine if the filler is being used effectively. In addition to orientation, aspect ratio, particle size

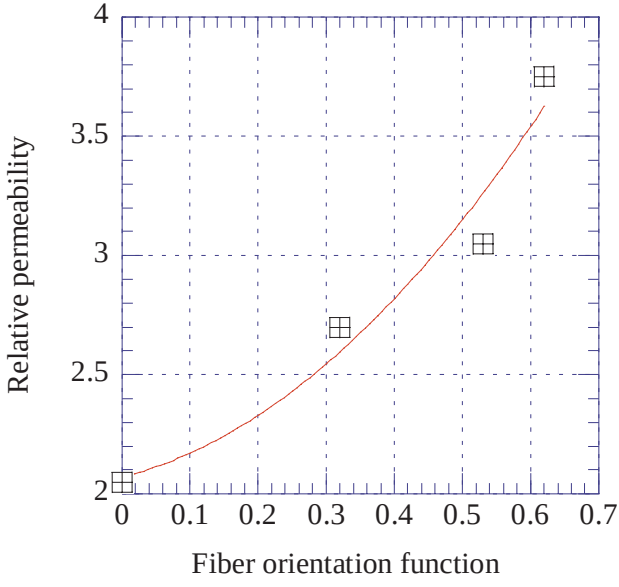

Figure 5.35. Relative permeability vs. nickel fiber orientation in HDPE matrix. [Adapted, by permission, from Fiske T, Gokturk H S, Yazici R, Kalyon D M, *Polym. Eng. Sci*., **37**, No.5, 1997, 826-37.]

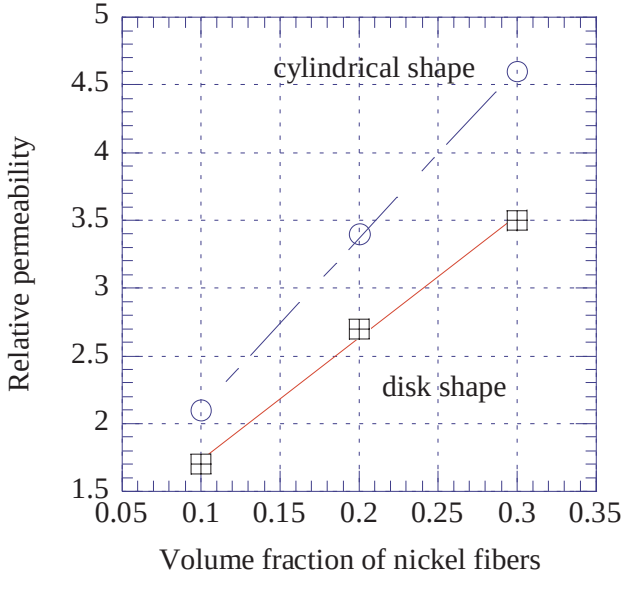

Figure 5.36. Relative permeability vs. volume fraction of nickel fibers in HDPE depending on article shape. [Adapted, by permission, from Fiske T, Gokturk H S, Yazici R, Kalyon D M, *Polym. Eng. Sci*., **37**, No.5, 1997, 826-37.]

and method of processing affect properties of manufactured materials with magnetic properties.

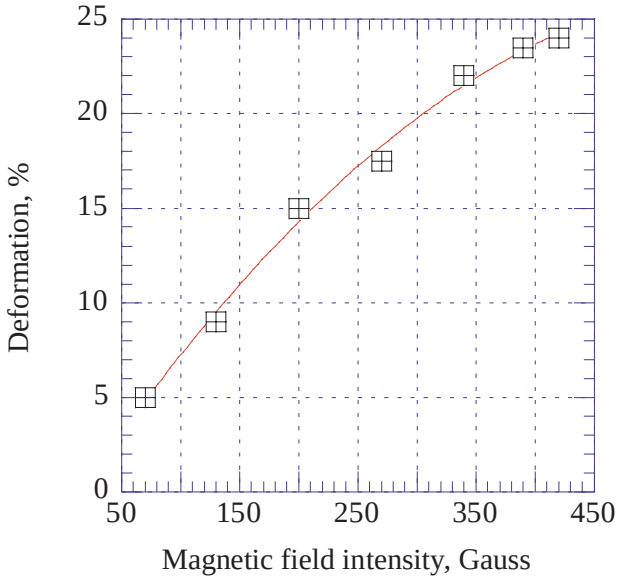

Figure 5.37. Deformation vs. magnetic field in polyacryloamide gel containing ferrite. [Adapted, by permission, from Klapcinski T, Galeski A, Kryszewski M, *J. Appl. Polym. Sci*., **58**, No.6, 1995, 1007-13.]

Figure 5.37 gives an interesting example of a magneto-mechanical device. Polyacrylamide gel containing ferrite was magnetized in compressed stage. Application of magnetic field causes deformation of gel depending on magnetic field intensity and *vice versa*.

REFERENCES

1 Gallas M R, Rosa A R, Costa T H, da Jornada J A H, *J. Mater. Res.,* **12**, No. 3, 1997, 764-8.
2 Coran A Y, Ignatz-Hoover F, Smakula P C, *Rubb. Chem. Technol*., **67**, No.2, 1994, 237-51.
3 Clarke J, Freakley P K, *Rubb. Chem. Technol*., **67**, No.4, 1994, 700-15.
4 Wampler W A, Rajeshwar K, Pethe R G, Hyer R C, Sharma S C, *J. Mat. Res*., **10**, No.7, 1995, 1811-22.
5 Schneider J P, Myers G E, Clemons C M, English B W, *J. Vinyl and Additive Technol*., **1**, No.2, 1995, 103-8.
6 Wang W D, Haidar B, Vidal A, Donnet J B, *Kaut. u. Gummi Kunst*., **47**, No.4, 1994, 238-41.
7 Ogadhoh S O, Papathanasiou T D, *Composites Part A: Applied Science and Manufacturing*, **27A**, No.1, 1996, 57-63.
8 Larena A, Pinto G, *Polym. Composites*, **16**, No.6, 1995, 536-41.
9 Golubev A I, *Int. Polym. Sci. Technol*., **22**, No.11, 1995, T/67-9.
10 Magrupov M A, Umarov A V, Saidkhodzhaeva K S, Kasimov G A, *Int. Polym. Sci. Technol*., **23**, No.1, 1996, T/77-9.
11 Kiselev V Y, Vnukova V G, *Int. Polym. Sci. Technol*., **23**, No.5, 1996, T/88-92.
12 Mushack R, Luttich R, Bachmann W, *Eur. Rubb. J.*, **178**, No.7, 1996, 24-9.
13 Jesionowski T, Krysztafkiewicz A, *Pigment Resin Technol*., **25**, No.3, 1996, 4-14.
14 Jones D W, Rizkalla A S, *J. Biomedical Materials Research (Applied Biomaterials)*, **33**, No.2, 1996, 89-100.
15 Weeling B, Electrical Conductivity in Heterogeneous Polymer Systems. Conductive Polymers, Conference Proceedings, 1992, Bristol, UK.
16 Itatani K, Yasuda R, Scott Howell F, Kishioka, *J. Mater. Sci*., **32**, 1997, 2977-84.
17 Kauly T, Keren B, Siegmann A, Narkis M, *J. Mater. Sci*., **32**, 1997, 693-9.

18 Tsagaropoulos G, Eisenberg A, *Macromolecules*, **28**, No.1, 1995, 396-8.
19 Maeda S, Armes S P, *Synthetic Metals*, **73**, No.2, 1995, 151-5.
20 Hegedus C R, Kamel I L, *J. Coatings Technol*., **65**, No.820, 1993, 31-43
21 Vratsanos L A, Farris R J, *Polym. Engng. Sci*., **33**, No.22, 1993, 1458-65.
22 Skelhorn D A, Antec '93. Conference Proceedings, New Orleans, La., 9th-13th May 1993, Vol. II, 1965-70.
23 Byers J T, Meeting of the Rubber Division, ACS, Cleveland, October 17-20, 1995, paper B.
24 Kovacevic V, Lucic S, Hace D, Glasnovic A, Smit I, Bravar M, *J. Adhesion*, **47**, No.1-3, 1994, 201-15.
25 Hornsby P R, Wang J, Cosstick K, Rothon R, Jackson G, Wilkinson G, Flame Retardants '94. Conference proceedings, London, 27th-28th January 1994, 93-108.
26 Maeda S, Armes S P, J. *Mat. Chem*., **4**, No.6, 1994, 935-42.
27 Zaborskaya L V, Dovgualo V A, Yurkevich O R, *J. Adhesion Sci. Technol*., **9**, No.1, 1995, 61-71.
28 Yoshinaga K, Hidaka Y, *Polym. J. (Jap.)*, **26**, No.9, 1994, 1070-9.
29 Gerspacher M, O'Farrel C P, Wampler W A, *Rubb. World*, **212**, No.3, 1995, 26-9.
30 Cha Y J, Choe S, *J. Appl. Polym. Sci*., **58**, No.1, 1995, 147-57.
31 Yu Long, Shanks R A, *J. Appl. Polym. Sci*., **61**, No.11, 1996, 1877-85.
32 Magee R W, *Rubb. Chem. Technol.*, **68**, No.4, 1995, 590-600.
33 Tan L S, McHugh, *J. Mater. Sci.*, **31**, 1996, 3701-6.
34 Pukanszky B, Voros G, *Polym.Composites*, **17**, No.3, 1996, 384-92.
35 Kovacevic V, Lucic S, Hace D, Glasnovic A, *Polym. Engng. Sci*., **36**, No.8, 1996, 1134-9.
36 Hashemi S, Din K J, Low P, *Polym. Engng. Sci*., **36**, No.13, 1996, 1807-20.
37 Mitsui S, Kihara H, Yoshimi S, Okamoto Y, *Polym. Engng. Sci*., **36**, No.17, 1996, 2241-6.
38 Lawandy S N, Botros S H, Darwish N A, Mounir A, *Polym. Plast. Technol. Engng*., **34**, No.6, 1995, 861-74.
39 Gorl U, Rausch R, Esch H, Kuhlmann R, *Int. Polym. Sci. Technol*., **23**, No.7, 1996, T/81-7.
40 Johnson K C, Antec '96. Volume III. Conference proceedings, Indianapolis, 5th-10th May 1996, 3545-9.
41 Stockblower D, Antec '96. Volume II. Conference proceedings, Indianapolis, 5th-10th May 1996, 1690-4.
42 Ishibashi J, Kobayashi A, Yoshikawa T, Shinozaki K, Antec '96. Vol. I. Conference Proceedings, Indianapolis, 5th-10th May 1996, 386-90.
43 Nguyen T N, Lethiecq M, Levassort F, Patat F, *Int. J. Polym. Analysis and Characterization*, **1**, No.4, 1995, 277-87.
44 Chen L, Liu K, Yang C Z, *Polym. Bull.*, **37**, No.3, 1996, 377-83.
45 Yoshinaga K, Iwasaki M, Teramoto M, Karakawa H, *Polym. & Polym. Composites*, **4**, No.3, 1996, 163-72.
46 Sanchez-Solis A, Estrada M R, *Polym. Degradat. Stabil*., **52**, No.3, 1996, 305-9.
47 Minkova L, *Coll. Polym. Sci*., **272**, No.2, 1994, 115-20.
48 Svistkov A L, *Polym. Sci*., **36**, No.3, 1994, 337-41.
49 Canova L A, Antec '93. Conference Proceedings, New Orleans, La., 9th-13th May 1993, Vol. II, 1943-9.
50 Herd C R, Meeting of the Rubber Division, ACS, Montreal, May 5-8, 1996, paper B.
51 Bergado S, *Plast. Compounding*, **17**, No.7, 1994, 32-8.
52 Garncarek Z, Piasecki R, Borecki J, Maj A, Sudol M, *J. Phys. D*, **29**, No.5, 1996, 1360-6.
53 Scaffaro R, Pedretti U, La Mantia F P, *Eur. Polym. J*., **32**, No.7, 1996, 869-75.
54 Averous L, Quantin J C, Lafon D, Crespy A, *Int. J. Polym. Analysis and Characterization*, **1**, No.4, 1995, 339-47.
55 Kretzschmar B, *Kunststoffe Plast Europe*, **86**, No.4, 1996, 20-2.
56 Donnet J B, Custodero E, Wang T K, *Kaut. u. Gummi Kunst*., **49**, No.4, 1996, 274-9.
57 Meijerink J I, Eguchi S, Ogata M, Ishii T, Amagi S, Numata S, Sashima H, *Polymer*, **35**, No.1, 1994, 179-86.
58 Donnet J B, *Kaut. u. Gummi Kunst*., **47**, No.9, 1994, 628-32.
59 Jarvela P A, Jarvela P K, *J. Mat. Sci.,* **31**, No.14, 1996, 3853-60.
60 Arakawa K, Iwami E, Kimura K, Nomaguchi K, *J. Reinf. Plast. Comp*., **13**, No.12, 1994, 1100-15.
61 Gent A N, Lai S-M, *Rubb. Chem. Technol*., **68**, No.1, 1995, 13-25.
62 Hjelm R P, Wampler W A, Seeger P A, Gerspacher M, *J. Mat. Res*., **9**, No.12, 1994, 3210-22.
63 Srinivasan G, Reneker D H, *Polym. Int*., **36**, No.2, 1995, 195-201.
64 Wada N, Uchiyama Y, *Int. Polym. Sci. Technol*., **21**, No.10, 1994, T/23-34.

65 Dzenis Y A, Reneker D H, Tsukruk V V, Patil R, *Composite Interfaces*, **2**, No.4, 1994, 307-19.
66 Al-Turaif H, Unertl W N, Lepoutre P, *J. Adhesion Sci. Technol*., **9**, No.7, 1995, 801-11.
67 Donnet J B, Tong Kuan Wang, *Macromol. Symp*., **108**, 1996, 97-109.
68 Donnet J B, Wang T K, *Prog. Rubb. Plast. Technol*., **11**, No.4, 1995, 261-7.
69 Okel T A, Waddell W H, *Rubb. Chem. Technol*., **68**, No.1, 1995, 59-76.
70 Wang M-J, Wolff S, Tan E-H, *Rubb. Chem. Technol*., **66**, No.2, 1993, 178-95.
71 Wolff S, Wang M-J, Tan E-H, *Rubb. Chem. Technol*., **66**, No.2, 1993, 163-77.
72 Byung Suk Jin, Kwang Hee Lee, Chul Rim Choe, *Polym. Int*., **34**, No.2, 1994, 181-5.
73 Molesky F, Schultz R, Midgett S, Green D, *J. Vinyl Additive Technol*., **1**, No.3, 1995, 159-61.
74 Vidal A, Wang W, Donnet J B, *Kaut. u. Gummi Kunst*., **46**, No.10, 1993, 770-8.
75 Probst N, Smet H, *Kaut. u. Gummi Kunst*., **48**, No.7-8, 1995, 509-11.
76 Agarwal S, Campbell G A, Antec 95. Volume I. Conference proceedings, Boston, Ma., 7th-11th May 1995, 839-42.
77 Cochet P, Barruel P, Barriquand L, Grobert J, Bomal Y, Prat E, IRC '93/144th Meeting, Fall 1993. Conference Proceedings, Orlando, Fl., 26th-29th Oct.1993, Paper 162.
78 Nasr G M, Badawy M M, Gwaily S E, Shash N M, Hassan H H, *Polym. Degradat. Stabil.,* **48**, No.2, 1995, 237-41.
79 Allen N S, Edge M, Corrales T, Childs A, Liauw C, Catalina F, Peinado C, Minihan A, *Polym. Degradat. Stabil*., **56**, 1997, 125-39.
80 Wolff S, *Rubb.Chem.Technol*., **69**, No.3, 1996, 325-46.
81 Papathanasiou T D, Lee P D, *Polym. Composites*, **18**, No.2, 1997, 242-53.
82 Grohens Y, Schultz J, *Int. J. Adhesion Adhesives*, **17**, 1997, 163-7.
83 Nago S, Mizutani Y, *J. Appl. Polym. Sci*., **53**, No.12, 1994, 1579-87.
84 Shiroki Y, *Int. Polym. Sci. Technol*., **20**, No.6, 1993, T/12-21.
85 Luzinov I, Voronov A, Minko S, Kraus R, Wilke W, Zhuk A, *J. Appl. Polym. Sci*., **61**, No.7, 1996, 1101-9.
86 Nago S, Mizutani Y, *J. Appl. Polym. Sci*., **61**, No.1, 1996, 31-5.
87 Jin-Shy Tsai, *Polym. Engng. Sci*., **35**, No.16, 1995, 1313-6.
88 Wu J, Lerner M M, *Chem. of Mat.*, **5**, No.6, 1993, 835-8.
89 Schueler R, Petermann J, Schulte K, Wentzel H P, *Macromol. Symp.,* **104**, 1996, 261-8.
90 Bomal Y, Godard P, *Polym. Engng. Sci*., **36**, No.2, 1996, 237-43.
91 Li Y, Wang M J, Zhang T, Zhang F, Fu X, *Rubb. Chem. Technol*., **67**, No.4, 1994, 693-9.
92 Baranovskii V M, Tarara A M, Khomik A A, *Int. Polym. Sci. Technol*., **20**, No.1, 1993, T/98-9.
93 Liauw C M, Lees G C, Hurst S J, Rothon R N, Dobson D C, *Plast. Rubb. Comp. Process. Appln*., **24**, No.4, 1995, 211-9.
94 Vogeler T, Kreuzer M, Tschudi T, Simoni F, *Molecular Crystals & Liquid Crystals*, **282**, 1996, 419-28.
95 Kovacevic V, Lucic S, Hace D, Cerovecki Z, *J. Adhesion Sci. Technol*., **10**, No.12, 1996, 1273-85.
96 Gruber T C, Zerda T W, Gerspacher M, *Rubb. Chem. Technol*., **67**, No.2, 1994, 280-7.
97 Maas S, Gronski W, *Kaut. u. Gummi Kunst*., **47**, No.6, 1994, 409-15.
98 Li Q, Manas-Zloczower I, Feke D L, *Rubb. Chem. Technol*., **69**, No.1, 1996, 8-14.
99 Qi Li, Feke D L, Manas-Zloczower I, *Rubb. Chem. Technol*., **68**, No.5, 1995, 836-41.
100 Potente H, Flecke J, Antec '96. Vol. I. Conference Proceedings, Indianapolis, 5th-10th May 1996, 178-82.
101 Eisenbach C D, Ribbe A, Goeldel A, *Kaut. u. Gummi Kunst.*, **49**, No.6, 1996, 406-10.
102 Foster J K, Sims E S, Venable S W, *Paint & Ink Int*., **8**, No.3, 1995, 18-21.
103 Long Y, Shanks R A, Antec '96. Volume III. Conference proceedings, Indianapolis, 5th-10th May 996, 3673-5
104 Wolff S, Wang M J, Tan E H, *Kaut. u. Gummi Kunst*., **47**, No.12, 1994, 873-84.
105 Tokita N, Shieh C H, Ouyang G B, Patterson W J, *Kaut. u. Gummi Kunst*., **47**, No.6, 1994, 416-20.
106 Maas S, Gronski W, *Rubb. Chem. Technol*., **68**, No.4, 1995, 652-9.
107 Lin C R, Lee Y D, *Macromol. Theory & Simulations*, **5**, No.6, 1996, 1075-104.
108 Miano F, Rabaioli M R, *Coll. & Surfaces*, **84**, Nos.2/3, 1994, 229-37.
109 Sudduth R D, *J. Appl. Polym. Sci*., **54**, No.9, 1994, 1243-62.
110 Hedgus C R, Kamel I L, *J. Coatings Technol.*, **65**, No.821, June 1993, 49-61
111 Boehm G G A, Nguyen M N, *J. Appl. Polym. Sci.*, **55**, No.7, 1995, 1041-50.
112 Molphy M, Mainwaring D E, Rizzardo E, Gunatillake P A, Laslett R L, *Polym. Int*., **37**, No.1, 1995, 53-61.
113 Chaturvedi M, Antec '97. Conference proceedings, Toronto, April 1997, 1865-8.

114 Rockenbauer A, Korecz L, Pukanszky B, *Polym. Bull*., **33**, No.5, 1994, 585-9.
115 Zhong-Fu Li, Grubb D T, Phoenix S L, *Composites Sci. & Technol*., **54**, No.3, 1995, 251-66.
116 Guanghong Lu, Xiaotian Li, Hancheng Jiang, *Composites Sci. & Technol*., **56**, No.2, 1996, 193-200.
117 Hashemi S, Gilbride M T, Hodgkinson J, *J. Mat. Sci.*, **31**, No.19, 1996, 5017-25.
118 Mayadunne A, Bhattacharya S N, Kosior E, Boontanjai C, Antec 95. Volume I. Conference proceedings, Boston, Ma., 7th-11th May 1995, 1178-82.
119 Godard P, Bomal Y, Biebuyck J J, *J. Mat. Sci*., **28**, No.24, 1993, 6605-10.
120 Ye B S, Svenson A L, Bank L C, *Composites*, **26**, No.10, 1995, 725-31.
121 Shiga T, Okada A, Kurauchi T, *J. Appl. Polym. Sci.*, **58**, No.4, 1995, 787-92.
122 Jancar J, *Macromol. Symp*., **108**, 1996, 163-72.
123 Golubev A I, *Int. Polym. Sci. Technol*., **22**, No.10, 1995, T/40-1.
124 Golubev A I, *Int. Polym. Sci. Technol*., **22**, No.10, 1995, T/42-3.
125 Konstantellos B, Sideridis E, *Coll. Polym. Sci*., **273**, No.4, 1995, 307-16.
126 Agari Y, Ueda A, Nagai S, *J. Appl. Polym. Sci*., **52**, No.9, 1994, 1223-31.
127 Ming Qiu Zhang, Jia Rui Xu, Han Ming Zeng, Qun Huo, Zhi Yi Zhang, Feng Chun Yun, Friedrich K, *J. Mat. Sci*., **30**, No.17, 1995, 4226-32.
128 Hoy L L, *J. Coatings Technol*., **68**, No.853, 1996, 33-9.
129 Qiu Q, Kumosa M, *Composites Sci. Technol,* **57**, 1997, 497-507.
130 Lee D H, Condrate R A, Reed J S, *J. Mater. Sci*., **32**, 1997, 471-8.
131 Liphard M, Von Rybinski W, Schreck B, *Prog. Coll. & Polym. Sci*., **95**, 1994, 168-74.
132 Yoshinaga K, Nakanishi K, Hidaka Y, Karakawa H, *Composite Interfaces*, **3**, No.3, 1995, 231-41.
133 Dupraz A M P, de Wijn J R, v. d. Meer S A T, de Groot K, *J. Biomed. Mat. Res*., **30**, No.2, 1996, 231-8.
134 **Kronos. Titanium Dioxide Pigments in Industrial Coatings**. *Kronos*, Leverkusen, 1996, DS 1805E/6965E.
135 Tang L-G, Kardos J L, *Polym. Composites*, **18**, No.1, 1997, 100-13.
136 Balard H, Papirer E, *Prog. Org. Coatings*, **22**, No.1-4, 1993, 1-17.
137 Zaborski M, Slusarski L, Vidal A, *Int. Polym. Sci. Technol*., **20**, No.11, 1993, T/99-104.
138 Pukanszky B, Belina K, Rockenbauer A, Maurer F H J, *Composites*, **25**, No.3, 1994, 205-14.
139 Zaborski M, Slusarski L, *Composite Interfaces*, **3**, No.1, 1995, 9-22.
140 Zumbrum M A, *J. Adhesion*, **46**, Nos.1-4, 1994, 181-96.
141 Donnet J B, Wang W, Vidal A, Wang M J, *Kaut. u. Gummi Kunst*., **4**6, No.11, Nov.1993, 866-71.
142 Wang W, Vidal A, Donnet J-B, Wang M-J, *Kaut. u. Gummi Kunst*., **46**, No.12, Dec.1993, 933-40.
143 Tsutsumi K, Ban K, Shibata K, Okazaki S, Kogoma M, *J. Adhesion*, **57**, Nos.1-4, 1996, 45-53.
144 Torro-Palau A, Fernandez-Garcia J C, Orgiles-Barcelo A C, Martin-Martinez J M, *J. Adhesion*, **57**, Nos.1-4, 1996, 203-25.
145 Asai S, Sumita M, *J. Macromol. Sci. B,* **34**, No.3, 1995, 283-94.
146 Rammoorthy M, Muzzy J, Antec '97. Conference proceedings, Toronto, April 1997, 2500-4.
147 Tsubokawa N, Seno K, *J. Macromol. Sci. A*, **31**, No.9, 1994, 1135-45.
148 Schreiber H P, Antec '95. Vol. II. Conference Proceedings, Boston, Ma., 7th-11th May 1995, 2446-51.
149 Ou Y C, Zhu J, Feng Y P, *J. Appl. Polym. Sci*., **59**, No.2, 1996, 287-94.
150 Mele P, Alberola N D, *Composites Sci. & Technol*., **56**, No.7, 1996, 849-53.
151 Shang S W, Williams J W, Soderholm K J M, *J. Mat. Sci.,* **30**, No.17, 1995, 4323-34.
152 Pak S H, Caze C, *J. Appl. Polym. Sci*., **65**, 1997, 143-53.
153 Bosse F, Schreiber H P, Eisenberg A, *Macromolecules*, **26**, No.24, 1993, 6447-54.
154 Hegedus C R, Kamel I L, J. *Coatings Technol*., **65**, No.820, 1993, 23-30.
155 Bataille P, Mahlous M, Schreiber H P, *Polym. Engng. Sci*., **34**, No.12, 1994, 981-5.
156 Ulkem I, Bataille P, Schreiber H P, *J. Macromol. Sci. A*, **31**, No.3, 1994, 291-303.
157 Persson A L, Bertilsson H, *Composite Interfaces*, **3**, No.4, 1996, 321-32.
158 Lee M C H. **Adhesive Chemistry - Development and Trends**. *Plenum*, New York, 1985.
159 Lee M C H, *J. Appl. Polym. Sci*., **33**, 1987, 2479.
160 Selzer R, Friedrich K, *Composites, Part A*, **28A**, 1997, 595-604.
161 Akay M, Mun S K A, Stanley A, *Composites Sci. Technol,* **57**, 1997, 565-71.
162 Kouloumbi N, Tsangaris G M, Kyvelidis S T, *J. Coatings Technol*., **66**, No.839, 1994, 83-8.
163 Hansen H, Polymers, Laminations & Coatings Conference, 1995, 653-8.
164 Evans L R, Meeting of the Rubber Division, ACS, Montreal, May 5-8, 1996, paper D.
165 Wang J Y, Ploehn H J, *J. Appl. Polym. Sci.*, **59**, No.2, 1996, 345-57.
166 Connor C, Chadwick M M, *J. Mat. Sci.,* **31**, No.14, 1996, 3871-7.

167 Akelah A, Moet A, *J. Mat. Sci*., **31**, No.13, 1996, 3589-96.
168 Rebouillat S, Escoubes M, Gauthier R, *J. Adhesion Sci. Technol*., **10**, No.7, 1996, 635-50.
169 Bauman B D, Plastics Finishing: Responding to Tomorrow's Global Requirements. Retec proceedings, Detroit, Mi, 21st-22nd March 1995, 62-73.
170 Gassan J, Bledzki A K, *Polym. Composites*, **18**, No.2, 1997, 179-84.
171 Darmstadt H, Roy C, Kaliaguine S, Sahouli B, Blacher S, Pirard R, Brouers F, *Rubb. Chem. Technol*., **68**, No.2, 1995, 330-41.
172 Bogoeva-Gaceva G, Burevski D, Dekanski A, Janevski A, *J. Mat. Sci*., **30**, No.13, 1995, 3543-6.
173 Zaborski M, Slusarski L, Vidal A, *Polim. Tworz. Wielk*., **38**, No.6, 1993, 263-8.
174 Zaborski M, Vidal A, Papirer E, *Polim. Tworz. Wielk*., **38**, No.7, 1993, 319-26.
175 Burnside S D, Giannelis E P, *Chem. of Mat.*, **7**, No.9, 1995, 1597-600.
176 Nasr G M, Badawy M M, *Polym. Test*., **15**, No.5, 1996, 477-84.
177 Lekatou A, Faidi S E, Lyon S B, Newman R C, *J. Mat. Res*., **11**, No.5, 1996, 1293-304.
178 Fatoev I I, Sitamov S, Manin V N, *Int. Polym. Sci. Technol*., **22**, No.9, 1995, T/26-8.
179 Budtov V P, Gandel'sman M I, Mulin Yu A, Suleimanov I E, Shterenzon A L, *Polym. Sci., Ser. A*, **37**, No.10, 1995, 1064-70.
180 Unnikrishnan G, Thomas S, Varghese S, *Polymer*, **37**, No.13, 1996, 2687-93.
181 Ou Y C, Yu Z Z, Vidal A, Donnet J B, *J. Appl. Polym. Sci*., **59**, No.8, 1996, 1321-8.
182 Addad J P C, Frebourg P, *Polymer*, **37**, No.19, 1996, 4235-42.
183 Xu P, Mark J E, *Eur. Polym. J*., **31**, No.12, 1995, 1191-5.
184 Ismail H, Freakley P K, Sutherland I, Sheng E, *Eur. Polym. J*., **31**, No.11, 1995, 1109-17.
185 Abdel-Aziz M M, Youssef H A, El Miligy A A, Yoshii F, Makuuchi K, *Polym. & Polym. Composites*, **4**, No.4, 1996, 259-68.
186 Younan A F, Choneim A M, Tawfik A A A, Abd-El-Nour K N, *Polym. Degradat. Stabil*., **49**, No.2, 1995, 215-22.
187 Strauss M, Kilian H G, Freund B, Wolff S, *Coll. Polym. Sci.*, **272**, No.10, 1994, 1208-17.
188 de Sena Affonso J E, Nunes R C R, *Polym. Bull*., **34**, No.5/6, 1995, 669-75.
189 Abdel-Aziz M M, Gwaily S E, *Polym. Degradat. Stabil*., **55**, 1997, 269-74.
190 Hegedus C R, Kamel I L, *J. Coatings Technol*., **65**, No.822, July 1993, 37-43.
191 Lan T, Kaviratna D, Pinnavaia T J, *Chem. of Mat*., **6**, No.5, 1994, 573-5.
192 Nakamura S, Kaneko S, Mizutani Y, *J. Appl. Polym. Sci.*, **49**, No.1, 1993, 143-50.
193 Duval J M, Kemperman A J B, Folkers B, Mulder M H V, Desgrandchamps G, Smolders C A, *J. Appl. Polym. Sci.,* **54**, No.4, 1994, 409-18.
194 Rabello M S, White J R, *Polym. Composites*, **17**, No.5, 1996, 691-704.
195 Gill T S, Xanthos M, Wirsbo Co., Antec '96. Volume II. Conference proceedings, Indianapolis, 5th-10th May 1996, 1757-61.
196 Xanthos M, Grenci J, Dagli S S, Antec '95. Vol.II. Conference Proceedings, Boston, Ma., 7th-11th May 1995, 3194-200.
197 Gill T S, Xanthos M, *J. Vinyl and Additive Technol*., **2**, No.3, 1996, 248-52.
198 Domka L, *Coll. Polym. Sci*., **272**, No.10, 1994, 1190-202.
199 Krysztafkiewicz A, Rager B, Maik M, Szymanowski J, *Coll. Polym. Sci*., **272**, No.12, 1994, 1526-35.
200 Hemenway C P, Latimer J J, *Tappi J*., **68** (5), 102 (1985).
201 Braun J H, *J. Coat. Technol.*, **63** (8), 1991, 43.
202 Schröder J, *Prog. Org. Coat*., **15**, 1988, 337.
203 Völz H G, *Prog. Org. Coat*., **18**, 1990, 289.
204 Braun J H, *J. Coat. Technol*., **62** (785), 1990, 39.
205 Parker A A, Martin E S, Clever T R, *J. Coatings Technol*., **66**, No.829, 1994, 39-46.
206 Godovsky D Yu, *Adv. Polym. Sci*., **119**, 1995, 81-122.
207 Athey R D, Kirkland T, Lindblom G, Swoboda J, *Eur. Coatings J.*, No.11, 1995, 793-8.
208 Murata N, Nishi S, Hosono S, *J. Adhesion*, **59**, Nos.1-4, 1996, 39-50.
209 Zhang C-Z, Liu W-M, Xue Q-J, Shen W-C, *J. Appl. Polym. Sci*., **66**, 1997, 85-93.
210 Lee I, *J. Mat. Sci*., **30**, No.23, 1995, 6019-22.
211 Shin Jen Shiao, Te Zei Wang, *Composites*, **27B**, No.5, 1996, 459-65.
212 Srivastava V K, Pathak J P, *Polym. & Polym. Composites*, **3**, No.6, 1995, 411-4.
213 Kuznezov A, Vasnev V, Gribova I, Krasnov A, Gureeva G, Ignatov V, *Int. J. Polym. Mat*., **32**, Nos.1-4, 1996. 85-91.
214 Bijwe J, *Polym. Composites*, **18**, No.3, 1997, 378-96.
215 White L, *Eur. Rubb. J.,* **177**, No.3, 1995, 27.

216 Yang A C M, *Polymer*, **35**, No.15, 1994, 3206-11.
217 Le Bras M, Bourbigot, Le Tallec Y, Laureyns J., *Polym. Degradat. Stabil*., **56**, 1997, 11-21.
218 Le Bras M, Bourbigot S, *Fire & Mat*., **20**, No.1, 1996, 39-49.
219 Miller B, *Plast. World*, **54**, No.12, 1996, 44-9.
220 Gibov K M, Mamleev V S, *J. Appl. Polym. Sci*., **66**, 1997, 329-38.
221 Ramani K, Vaidyanathan A, *J. Composite Mat*., **29**, No.13, 1995, 1725-40.
222 Baranovskii V M, Bondarenko S I, Kachanovskaya L D, Zelenev Y V, Makarov V G, Ovcharenko F D, *Int. Polym. Sci. Technol.*, **22**, No.1, 1995, T/91-3.
223 Ruiz F A, Polymers, Laminations & Coatings Conference, 1995, 647-51.
224 Bigg D M, **Thermal and Electrical Conductivity of Polymers Materials**, Eds. Godovsky Y K, Privalko V P, *Springer*, Berlin 1995.
225 Tavman I H, *J. Appl. Polym. Sci*., **62**, No.12, 1996, 2161-7.
226 Nyilas A, Rehme R, Wyrwich C, Springer H, Hinrichsen G, *J. Mat. Sci. Lett*., **15**, No.16, 1996, 1457-9.
227 Nasr G M, Badawy M M, Gwaily S E, Attia G, *Polym. Int*., **38**, No.3, 1995, 249-55.
228 Priss L S, *Int. Polym. Sci. Technol*., **23**, No.7, 1996, T53-6.
229 Oien H T, Polyurethanes '95. Conference Proceedings, Chicago, Il., 26th-29th Sept.1995, 137-41.
230 Okoroafor M O, Wang A, Bhattacharjee D, Cikut L, Haworth G J, Polyurethanes '95. Conference Proceedings, Chicago, Il., 26th-29th Sept.1995, 303-9.
231 Nichols K, Solc J, Shieu F, Antec '93. Conference Proceedings, New Orleans, La., 9th-13th May 1993, Vol. II, 1938-42.
232 McCabe J F, Wassell R W, *J. Mat. Sci. Mat. In Med*., **6**, No.11, 1995, 624-9.
233 Baranovskii V M, Bondarenko V V, Zadorina E N, Cherenkov A V, Zelenev Y V, *Int. Polym. Sci. Technol*., **23**, No.6, 1996, T/87-9.
234 Strumpler R, Maidorn G, Garbin A, Ritzer L, Greuter F, *Polym. & Polym. Composites*, **4**, No.5, 1996, 299-304.
235 Mamunya E P, Shumskii V F, Lebedev E V, *Polym. Sci*., **36**, No.6, 1994, 835-8.
236 Mateev M M, Totev D L, *Kaut. u. Gummi Kunst.*, **49**, No.6, 1996, 427-31.
237 Chan C M, *Polym. Engng. Sci*., **36**, No.4, 1996, 495-500.
238 Achour M E, El Malhi M, Miane J L, Carmona F, *J. Appl. Polym. Sci*., **61**, No.11, 1996, 2009-13.
239 Acosta J L, Jurado J R, *J. Appl. Polym. Sci*., **57**, No.4, 1995, 431-7.
240 Khan S A, Baker G L, Colson S, *Chem. of Mat*., **6**, No.12, 1994, 2359-63.
241 Ali M H, Abo-Hashem A, *Plast. Rubb. Comp. Process. Appln*., **24**, No.1, 1995, 47-51.
242 Bowen C P, Bhalla A S, Newnham R E, Randall C A, *J. Mat. Res*., **9**, No.3, 1994, 781-8.
243 Abramova N A, Diikova E U, Lyakhovskii Yu Z, *Polym. Sci*., **36**, No.9, 1994, 1308-9.
244 Mamunya E P, Davidenko V V, Lebedev E V, *Polym. Composites*, **16**, No.4, 1995, 319-24.
245 Lei Yang, Schruben D L, *Polym. Engng. Sci*., **34**, No.14, 1994, 1109-14.
246 Chellappa V, Chiou Z W, Jang B Z, Antec '94. Conference Proceedings, San Francisco, Ca., 1st-5th May 1994, Vol. II, p.2371-4.
247 Fiske T J, Gokturk H S, Kalyon D M, Antec '93. Conference Proceedings, New Orleans, La., 9th-13th May 1993, Vol. I, 614-7.
248 Gokturk H S, Fiske T J, Kalyon D M, Antec '93. Conference Proceedings, New Orleans, La., 9th-13th May 1993, Vol. I, 605-8.
249 Suri A, Min K, Antec '97. Conference proceedings, Toronto, April 1997, 1487-91.
250 Zaikin A Y, Nigmatullin V A, *Kaut. u. Gummi Kunst*., **47**, No.10, 1994, 709-14.
251 Soares B G, Gubbels F, Jerome R, Teyssie P, Vanlathem E, Deltour R, *Polym. Bull*., **35**, No.1/2, 1995, 223-8.
252 Svorcik V, Micek I, Jankovskij O, Rybka V, Hnatowicz V, Wang L, Angert N, *Polym. Degradat. Stabil*., **55**, 1997, 115-21.
253 Hao Tang, Xinfang Chen, Aoqing Tang, Yunxia Luo, *J. Appl. Polym. Sci*., **59**, No.3, 1996, 383-7.
254 Porter J R, Groseth C K, Little D W, Polyurethanes '95. Conference Proceedings, Chicago, Il., 26th-29th Sept.1995, 532-7.
255 Klason C, McQueen D H, Kubat J, *Macromol. Symp*., **108**, 1996, 247-60.
256 Trotignon J P, Tcharkhtchi A, *Macromol. Symp*., **108**, 1996, 231-45.
257 Modine F A, Duggal A R, Robinson D N, Churnetski E L, Bartkowiak M, Mahan G D, Levinson L M, *J. Mat. Res*., **11**, No.11, 1996, 2889-94.
258 Gregorio R, Cestari M, Bernardino F E, *J. Mat. Sci.*, **31**, No.11, 1996, 2925-30.
259 Svorcik V, Rybka V, Hnatowicz V, Bacakova L, *J. Mat. Sci. Lett*., **14**, No.24, 1995, 1723-4.
260 Dyrda V I, Meshchaninov S K, *Int. Polym. Sci. Technol*., **22**, No.12, 1995, T/14-6.

261 Chmutin I A, Ryvkina N G, Ponomarenko A T, Shevchenko V G, *Polym. Sci., Ser. A*, **38**, No.2, 1996, 173-7.
262 Kimura T, Asano Y, Yasuda S, *Polymer*, **37**, No.14, 1996, 2981-7.
263 Tang H, Chen X, Luo Y, *Eur. Polym. J.*, **32**, No.8, 1996, 963-6.
264 Roth S, Mair H J, *Int. Polym. Sci. Technol.*, **22**, No.11, 1995, T/1-6.
265 Hedvig P, *Int. Polym. Sci. Technol.*, **23**, No.3, 1996, T/23-8.
266 Stukhlyak P D, Shkodzinskii O K, Mytnik N M, Shovkun A P, Kovalyuk B P, *Int. Polym. Sci. Technol.*, **23**, No.6, 1996, T/81-4.
267 Wei Y, Sancaktar E, *J. Adhesion Sci. Technol.*, **10**, No.11, 1996, 1199-219.
268 Sethi R S, Goosey M T, London, *Chapman & Hall*, 1995, p.1-36. **Special Polymers for Electronics and Optoelectronics**, Chilton J A, Goosey M T, Ed.
269 Karasek L, Meissner B, Asai S, Sumita M, *Polym. J. (Jap.)*, **28**, No.2, 1996, 121-6.
270 Saad A L G, Younan A F, *Polym. Degradat. Stabil.*, **50**, No.2, 1995, 133-40.
271 Vasnev V A, Tarasov A I, Istratov V N, Ignatov V N, Krasnov A P, Kuznetsov A I, Surkova I N, *Reactive & Functional Polym.*, **26**, Nos.1-3, 1995, 177-83.
272 Narkis M, Tchoudakov R, Breuer O, Siegmann A, Antec '95. Vol. II. Conference Proceedings, Boston, Ma., 7th-11th May 1995, p.1343-6.
273 Fiske T, Gokturk H S, Yazici R, Kalyon D M, *Polym. Eng. Sci.*, **37**, No.5, 1997, 826-37.
274 Fiske T J, Gokturk H, Kalyon D M, *J. Appl. Polym. Sci.*, **65**, 1997, 1371-7.
275 Fiske T, Gokturk H S, Yazici R, Kalyon D M, Antec '97. Conference proceedings, Toronto, April 1997, 1482-6.
276 Klapcinski T, Galeski A, Kryszewski M, *J. Appl. Polym. Sci.*, **58**, No.6, 1995, 1007-13.
277 Yogo T, Nakamura T, Kikuta K, Sakamoto W, Hirano S, *J. Mat. Res.*, **11**, No.2, 1996, 475-82.
278 Stassen S, Cloots R, Vanderbemden P, Godelaine P A, Bougrine H, Rulmont A, Ausloos M, *J. Mat. Res.*, **11**, No.5, 1996, 1082-5.
279 Fiske T J, Gokturk H, Kalyon D M, Antec '96. Volume II. Conference proceedings, Indianapolis, 5th-10th May 1996, 1768-72.